L. Quartapelle, A. Muzzio
A Simple Thermodynamic Model of Diluted Hydrogen Gas/plasma for CFD Applications
European Physical Journal D, Vol. 69, N. 6, 156, 2015, 156 (17 pages)
doi:10.1140/epjd/e2015-60124-6

EPJ manuscript No.
(will be inserted by the editor)

A simple thermodynamic model of diluted hydrogen gas/plasma for CFD applications

L. Quartapelle[1a] and A. Muzzio[2]

[1] Dipartimento di Scienze e Tecnologie Aerospaziali, Politecnico di Milano
Via La Masa 34, 20156 Milano, Italy;

[2] Dipartimento di Energia, Politecnico di Milano
Via Lambruschini 4, 20156 Milano, Italy.

Received: date / Revised version: date

Abstract. This work describes a simple thermodynamic model of the hydrogen gas at low densities and for temperatures going from those involving quantum rotations of ortho- and para-hydrogen up to the fully ionized state. The closed-form energy levels of Morse rotating oscillator given in Harris and Bertolucci [14] (but not those in Morse's original paper) are shown to provide an internal partition function of H_2 that is a sufficiently accurate representation of that exploiting the state-of-the-art spectrum of roto-vibrational levels calculated by Pachucki and Komasa [13]. A system of two coupled quadratic equations for molecular dissociation and atomic ionization at thermodynamical and chemical equilibrium is derived according to the statistical mechanics by assuming that the system is an ideal mixture containing molecules, neutral atoms and noninteracting protons and electrons. The system of two equations reduces to a single quartic equation for the ionization unknown, with the coefficients dependent on the temperature and the specific volume. Explicit relations for specific energy and entropy of the hydrogen ideal gas/plasma model are derived. These fully compatible equations of state provide a complete thermodynamic description of the system, uniformly valid from low temperatures up to a fully ionized state, with electrons and ions relaxed to one and the same temperature. The comparison with results of other models developed in the framework of the physical and chemical pictures shows that the proposed elementary model is adequate for computational fluid dynamics purposes, in applications with the hydrogen gas under diluted conditions and when the dissociation and ionization can be assumed at thermodynamical and chemical equilibrium.

PACS. PACS-key 51.30.+i

1 Introduction

Monatomic ideal gases at low densities and for temperatures lower than the ionization energy are described properly by the pressure equation of state $PV = NkT$ together with the specific heat equation $c_v =$ constant, both derivable from a single fundamental thermodynamic relation $S = S(E, V, N)$, available in an explicit analytic form, see *e.g.*, [1, p. 373, eq. (16.73)]. Molecular gases do not admit a similar compact representation due to the presence of the internal rotational and vibrational modes. In the simplest case of a diatomic gas, molecular vibrations are often described within the harmonic approximation, by an infinite ladder of the uniformly distributed energy levels of the Einstein quantum oscillator, see [1, p. 336] or [2, p. 116]. This model yields a nonconstant specific heat c_v due to the temperature dependent vibrational contribution $c_v^{\mathrm{har}}(T) = R\left(\frac{T_\mathrm{v}}{T}\right)^2 \frac{\mathrm{e}^{T_\mathrm{v}/T}}{(\mathrm{e}^{T_\mathrm{v}/T}-1)^2}$, with T_v denoting the characteristic vibrational temperature of the molecule, which makes it impossible for the fundamental relation to be expressible explicitly in analytical form.

On the other hand, the harmonic model is conflicting with the possibility of molecular dissociation occuring at $T > T_\mathrm{v}$. This difficulty is attenuated in some models where $c_v^{\mathrm{har}}(T)$ is halved, as proposed by Lighthill [3], which corresponds to take the vibrational degrees of freedom of the molecules always half-excited at any temperature, see also [4, Sec. 5.3, p. 157]. A physically sounder procedure for overcoming the harmonic approximation consists in making recourse to the Morse potential [5] which accounts for the vibrational nonlinearity and allows for the molecular disintegration into atoms. The Morse vibrational spectrum is still discrete but with a nonuniform spacing of the energy levels of increasing density, and has a finite number of excited states, before the molecular dissociation. A thermodynamic model for diatomic gases based on the rotat-

Send offprint requests to:
[a] *e-mail address:* luigi.quartapelle@polimi.it

ing Morse oscillator was developed by Gordillo-Vázquez and Kunc [6] and was compared for several diatomic gases to that relying upon the Tietz–Hua rotating oscillator.

The molecular rotations present however an additional difficulty: rotations and vibrations are in principle coupled together. For most diatomic molecules, the moment of inertia is so large and the characteristic rotational temperature T_r so small, of the order of only a few kelvins, that the rotational states may be uncoupled from the vibrational ones. Consequently, the molecular rotations can be treated according to a semi-classical description of fully excited rigid rotations valid for $T > T_\mathrm{r}$, resulting in a constant contribution R to c_v. On the contrary, the hydrogen molecule H_2 (and its isotopes) has a very low moment of inertia, as noted by Landau & Lifshitz [7, p. 139], yielding the fairly high value $T_\mathrm{r} = 88\,\mathrm{K}$, so that the roto–vibration coupling must be taken into account.

In the range of high temperatures, say $T \gg 5000\,\mathrm{K}$, a thermodynamic description faces with another difficulty—hydrogen ionization. For this element, atomic ionization is most simple since the spectrum of the electron states around the proton nucleus is known exactly and can be used to compute the electronic contribution to the partition function of H. Unfortunately, the series diverges due to the long-range character of the electric interaction: therefore atomic ionization requires a subtler mathematical treatment than molecular dissociation. In principle, the equations of states of the ionized hydrogen gas can be derived by statistical mechanics starting from the complete Hamiltonian of the system, including the interaction energy between the charges, within the framework called physical picture, see, *e.g.*, the classical studies of Hummer, Mihalas and Däppen [8] and [9], or the work of Alastuey *et al.* [10] on exact results for the hydrogen plasma at low temperatures. Along the same rigorous lines, the recent work of Alastuey and Ballenegger [11] has derived the equations of state covering molecular, atomic and plasma phases by means of the Ebeling function and a new four body partition function.

Within a reduced setting, for low densities, say in the range $\rho < 1\,\mathrm{kg/m^3}$, the electrical charges are only weakly coupled, see, *e.g.*, [12, p. 216], and one may attempt to formulate a simpler thermodynamic model by assuming that, after ionization, all charges behave as noninteracting particles after a time long enough for the temperatures of electrons and ions to become equal.

The aim of this work is to present a complete thermodynamic description of the diluted hydrogen gas including the rotational–vibrational coupling active at low T, the molecular dissociation process occurring for $T > 1000\,\mathrm{K}$, and the atomic ionization which may occur for $T > 5000\,\mathrm{K}$. Consistent expressions for the specific energy and entropy of the gas/plasma system at thermodynamical and chemical equilibrium are derived in an explicit form, involving the internal partition function of the molecule H_2 and a suitable reduced version of the partition function of the hydrogen atom.

The former is first evaluated from the accurate numerical energy levels of all the roto-vibrational states before dissociation determined recently by Pachucki and Komasa including nonadiabatic corrections [13]. These energies are used here to compute the internal partition function needed to model molecular dissociation of H_2. An alternative closed-form expression for the roto-vibrational energy levels is also derived from the classical reference Harris&Bertolucci [14]. These energy levels differ from Morse's original ones [5] only for the term representing the interaction between rotations and vibrations. Rather unexpectedly, the Harris&Bertolucci spectrum is found to give the internal partition function H_2 notably different from that provided by Morse spectrum and a fairly accurate approximation to the partition function based on Pachucki and Komasa spectrum. The Harris&Bertolucci approximate spectrum is employed here to formulate a simple closed-form analytical model of the thermodynamic properties of the hydrogen gas, including dissociation and ionization, a result that seems to be new, to the best of our knowledge.

As far as the atomic partition function of H is concerned, its divergence is circumvented by means of a simple modification introduced originally by Fermi [15]. The entire analysis is conducted in the framework of the statistical mechanics of noninteracting particles. A final thermodynamic model is obtained which describes the hydrogen gas/plasma at equilibrium by means of fully compatible simple equations of state and is at the same time uniformly valid for any temperature in the limit of low density.

2 Molecular partition function

The starting assumption is that of an ideal gas according to the classical Maxwell–Boltzmann statistics. This is possible provided $\lambda_T \ll \left(\frac{V}{N}\right)^{1/3}$, where $\lambda_T = \frac{h}{(2\pi m k T)^{1/2}}$ is the thermal de Broglie wavelength and N is the number of identical particles of mass m contained in a volume V and at temperature T, see, *e.g.*, [1, p. 405]. The Helmholtz free energy F of a system of noininteracting particles consisting of N_{H_2} molecules and N_H atoms of hydrogen is [12, p. 185]

$$F(T, V, N_{\mathrm{H}_2}, N_\mathrm{H}) = -kT \ln \left(\frac{Z_{\mathrm{H}_2}^{N_{\mathrm{H}_2}}}{N_{\mathrm{H}_2}!} \frac{Z_\mathrm{H}^{N_\mathrm{H}}}{N_\mathrm{H}!} \right). \tag{2.1}$$

Such Helmholtz potential is based on the assumption that the gas is a mixture of ideally noninteracting molecules and neutral atoms, which holds only in the limit of a low density.

The partition functions of the hydrogen molecule H_2 and atom H in (2.1) are given respectively by

$$Z_{\mathrm{H}_2}(T, V) = Z_{\mathrm{H}_2}^{\mathrm{tr}}(T, V)\, Z_{\mathrm{H}_2}^{\mathrm{rv,nuc}}(T)\, Z_{\mathrm{H}_2}^{\mathrm{el}}(T), \tag{2.2}$$

$$Z_\mathrm{H}(T, V) = Z_\mathrm{H}^{\mathrm{tr}}(T, V)\, Z_\mathrm{H}^{\mathrm{nuc,el}}(T). \tag{2.3}$$

The translational partition function of the molecule is

$$Z_{\mathrm{H}_2}^{\mathrm{tr}}(T, V) = \left(\frac{m_{\mathrm{H}_2} k T}{2\pi\hbar^2} \right)^{\frac{3}{2}} V \tag{2.4}$$

and similarly for the atomic one $Z^{\mathrm{tr}}_{\mathrm{H}}(T,V)$, while

$$Z^{\mathrm{el}}_{\mathrm{H}_2}(T) = g^{\mathrm{el}}_{\mathrm{H}_2}\,\mathrm{e}^{-E_{\mathrm{H}_2,0}/kT}, \tag{2.5}$$

$$Z^{\mathrm{nuc,el}}_{\mathrm{H}}(T) = g^{\mathrm{n}}_{\mathrm{H}}\,g^{\mathrm{el}}_{\mathrm{H}}\,\mathrm{e}^{-E_{\mathrm{H},0}/kT}, \tag{2.6}$$

where $g^{\mathrm{n}}_{\mathrm{H}} = 2s_{\mathrm{H}} + 1 = 2$ is the multiplicity of the spin states of the atomic nucleus of H of spin $s_{\mathrm{H}} = \frac{1}{2}$ and g^{el} is the statistical weight of the electronic state. Furthermore, $E_{\mathrm{H}_2,0}$ and $E_{\mathrm{H},0}$ denote the ground state energy of hydrogen molecule and atom, respectively.

Due to the homonuclear nature of H_2, its internal partition function cannot be factored in a nuclear and a rotational part, cf. [2, p. 185]. Moreover, since rotations and vibrations are coupled together, they are considered jointly in the factor $Z^{\mathrm{rv,nuc}}_{\mathrm{H}_2}(T)$. By summarizing, the complete partition functions of the molecule and the atom will be, respectively,

$$Z_{\mathrm{H}_2}(T,V) = \left(\frac{m_{\mathrm{H}_2}kT}{2\pi\hbar^2}\right)^{\frac{3}{2}} Z^{\mathrm{rv,nuc}}_{\mathrm{H}_2}(T)\,g^{\mathrm{el}}_{\mathrm{H}_2}\,\mathrm{e}^{-E_{\mathrm{H}_2,0}/kT}\,V, \tag{2.7}$$

$$Z_{\mathrm{H}}(T,V) = \left(\frac{m_{\mathrm{H}}kT}{2\pi\hbar^2}\right)^{\frac{3}{2}} g^{\mathrm{n}}_{\mathrm{H}}\,g^{\mathrm{el}}_{\mathrm{H}}\,\mathrm{e}^{-E_{\mathrm{H},0}/kT}\,V. \tag{2.8}$$

The internal partition function of the diatomic molecule must include a summation over its different electronic states, and the summations over the rotational and vibrational states, which are both dependent on the electronic configuration, see, *e.g.*, Babou *et al.* [16]. Initially, one can consider only the ground state of the molecule and disregard any electronic excitation. This assumption is used to simplify the analysis but it could be removed by including later higher electronic states of the molecule in each roto-vibrational state. By taking into account the combined effect of the multiplicity of the hydrogen nuclear spin $s_{\mathrm{H}} = \frac{1}{2}$ and of the degeneracy of the rotational quantum number $j = 0, 1, \ldots$ through the coefficient $\Delta_j \equiv \big[2 - (-1)^j\big](2j+1)$, the internal partition function of the hydrogen molecule is assumed in the following form

$$Z^{\mathrm{rv,nuc}}_{\mathrm{H}_2}(T) = \sum_{j=0}^{J_{\max}} \Delta_j \sum_{n=0}^{N_j} \mathrm{e}^{-E_{j,n}/kT}, \tag{2.9}$$

where $n = 0, 1, \ldots$, is the vibrational quantum number of the molecule, $E_{j,n}$ denotes the energy of the roto-vibrational state (j,n) and N_j indicates the maximum number of vibrational states which are possible for a fixed rotation state j. The external sum in (2.9) when limited to j even or to j odd gives the para- and ortho-hydrogen, respectively. To evaluate this function, the upper bound $J_{\max}$ for j of the outer sum and that N_j for n of the inner sum must be known.

The values $E_{j,n}$ of H_2 are taken from the work of Pachucki and Komasa [13], where $J_{\max} = 31$ and $N_j = 14, 13, \ldots, 1, 0$, for $j = 0, 1, \ldots, 31$, with some repetitions in the N_j values. In Figure 1 we plot the function $z_{\mathrm{rv}}(T) = \mathrm{e}^{-D_e/kT} Z^{\mathrm{rv,nuc}}_{\mathrm{H}_2}(T)$, which should be indicated more precisely by $z^{\mathrm{nuc}}_{\mathrm{rv}}(T)$. The energy D_e is the depth of the empirical Morse potential [5]

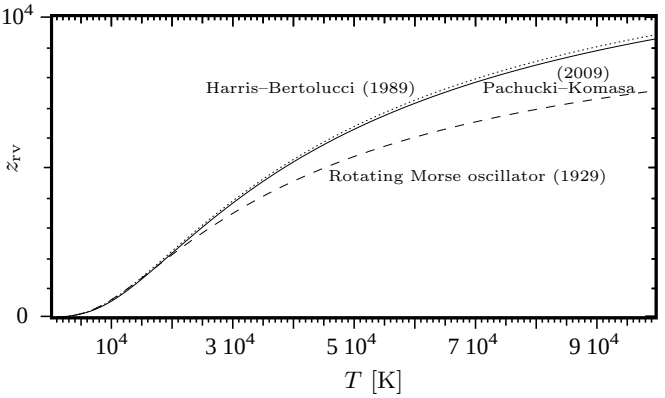

Fig. 1. Internal partition function $z_{\mathrm{rv}}(T)$ of H_2 for different roto-vibrational spectra. Continuous line: numerical energy levels of Pachucki and Komasa [13]. Dotted curve: closed-form approximate spectrum (2.12) of Harris and Bertolucci [14]. Dashed curve: closed-form approximate spectrum (2.20) of Morse [5].

$$V(r) = D_e\big[\big(1 - \mathrm{e}^{-\beta(r-r_e)}\big)^2 - 1\big], \tag{2.10}$$

where r is the internuclear distance, r_e is its equilibrium value and β^{-1} is the length scale of the Morse elastic force. The values for the hydrogen molecules are given in Tables 1 and 2 and $D_e = 4.75\,\mathrm{eV}$. The continuous curve of Figure 1 represents the partition function based on the full finite set of accurate dissociation energy values for 301 roto-vibrational states of the ground state ${}^1\Sigma^+_g$ calculated in [13], before the molecule disintegrates.

It is interesting to compare this partition function with the one provided by approximate analytical solutions to the Schrödinger equation for the nuclear motion with the effective Morse potential $V^{\mathrm{eff}}_j(r) = V(r) + \frac{\hbar^2}{2\mu}\frac{j(j+1)}{r^2}$ which includes the centrifugal rotational term of the molecule, μ being its reduced mass. In particular, the energy levels can be expressed in closed form according to the energy spectrum given in Harris and Bertolucci [14, p. 115, eq. (3.45)], see also Blake [17, p. 56, eq. (7.11)]. The expression is made transparent by introducing the dimensionless parameters

$$\chi_e \equiv \frac{\hbar\beta}{\sqrt{2\mu D_e}} \qquad \text{and} \qquad \kappa \equiv \frac{1}{\beta r_e}, \tag{2.11}$$

the former being twice the usual anharmonicity constant $x_e = \chi_e/2$. In terms of these parameters, the complete expression of the Harris–Bertolucci approximate spectrum reads

$$\begin{aligned}\frac{E^{\mathrm{HB}}_{j,n}}{D_e} = -1 &+ \big[1 - j(j+1)(\kappa^2\chi_e)^2\big]j(j+1)(\kappa\chi_e)^2 \\ &+ \big[2 - \big(n+\tfrac{1}{2}\big)\chi_e\big]\big(n+\tfrac{1}{2}\big)\chi_e \\ &- 3j(j+1)\big(n+\tfrac{1}{2}\big)(1-\kappa)(\kappa\chi_e)^3.\end{aligned} \tag{2.12}$$

Table 1. Morse parameters of H_2 [18].

	μ (amu)	β (Å^{-1})	β^{-1} (Å)	r_e (Å)	$\kappa = 1/\beta r_e$
H_2	0.504	1.905	0.525	0.741	0.7085

Table 2. Other Morse parameters for H_2 [18].

	χ_e	$N_{\max}$	D_e (eV)	U (eV)
H_2	0.0571	17	4.75	4.48

Table 3. Characteristic temperatures of H_2 in K.

	$T_{\rm cr}$	$T_{\rm r}$	$T_{\rm v}$	T_D	$T_{\rm i}$
H_2	33.04	88.3	6300	55 121	157 800

The internal partition function based on the Harris–Bertolucci spectrum will be written in the following form

$$z_{\rm rv}^{\rm HB}(T) = \sum_{j=0}^{J_{\max}} \Delta_j \, \mathrm{e}^{-b_j T_{\rm r}/T} \sum_{n=0}^{N_j} \mathrm{e}^{-a_n^j T_{\rm v}/T}, \qquad (2.13)$$

where $kT_{\rm r} = \epsilon_{0,\rm r} = \hbar^2/(2\mu r_e^2)$ and $kT_{\rm v} = \hbar\omega_e = 2D_e\chi_e$. In this form of the sum, an exponential term dependent only on the angular quantum number j and the rotational temperature $T_{\rm r}$ is factored out from the internal sum on the vibrational states. The coefficients in the exponentials are given by the approximate spectrum (2.12) and are found to be

$$a_n^j = \Big[1 - \big(n+\tfrac12\big)\tfrac{\chi_e}{2} - 3j(j+1)(1-\kappa)\,\kappa\chi_e \tfrac{T_{\rm r}}{T_{\rm v}}\Big]\big(n+\tfrac12\big), \qquad (2.14)$$

$$b_j = \big[1 - j(j+1)(\kappa^2\chi_e)^2\big] j(j+1), \qquad (2.15)$$

for $0 \le j \le J_{\max}$ and $0 \le n \le N_j$, with $J_{\max}$ and N_j to be defined below. Notice the occurrence of the temperature ratio $T_{\rm r}/T_{\rm v}$ as a factor in the term coupling rotations with vibrations. Thanks to the factor $T_{\rm r}/T_{\rm v}$, the evaluation of $z_{\rm rv}^{\rm HB}(t)$ with the inner summation on n and the outer on j turns out to be more stable numerically than the other way around. We notice in passing that the rotational–vibrational coupling has been found to be important in the determination of volume viscosity in H–H_2 mixtures by Bruno, Esposito and Giovangigli [19].

To define the upper bounds in the two sums of (2.13) it is necessary to establish a cutoff for the admissible values of j and n, within the considered approximation of the spectrum. For the nonrotating Morse oscillator, *i.e.*, for $j = 0$, the maximum vibrational mode is easily found to be $N_{\max} = 1/\chi_e - (1/2)$. According to the nonrotating Morse model, vibrational states with $n > N_{\max}$ are impossible: the molecule disappears and is replaced by its two constituent atoms. When rotations are allowed within the empirical Morse model, the limit of molecular existence depends on the rotational state and can be defined by the stationarity of the energy of the vibro-rotational levels. In particular, by continuity, at low rotational numbers j the energy stationarity will be achieved by $\partial E_{j,n}/\partial n = 0$, a criterion employed also in [16, p. 420]. However, for the energy levels (2.12) of H_2 at higher j this derivative does not vanish and a cutoff is attainable only via the stationarity at fixed n, namely by the condition $\partial E_{j,n}/\partial j = 0$. Thus, the curve of energy stationarity that delimits the region of allowed quantum states before the hydrogen molecule breaks into atoms consists of two portions, associated with the conditions $\partial E_{j,n}/\partial n = 0$ or $\partial E_{j,n}/\partial j = 0$, respectively. One finds the bounds of n for fixed j

$$\begin{aligned} N^{\rm vib}(j) &= N_{\max} - \tfrac32(1-\kappa)\kappa^3\chi_e j(j+1), \\ N^{\rm rot}(j) &= \frac{1}{3(1-\kappa)\kappa\chi_e} - \frac12 - \frac{2\kappa^3\chi_e}{3(1-\kappa)}\, j(j+1). \end{aligned} \qquad (2.16)$$

The range of the rotational quantum number j is limited by the maximum values $J_{\max}^{\rm vib}$ and $J_{\max}^{\rm rot}$ which are obtained by solving the equations $N^{\rm vib}(j) = 0$ and $N^{\rm rot}(j) = 0$ for j, respectively. The latter are simple quadratic equations of the type $j(j+1) + \text{constant} = 0$, cf. [6]. Then we define

$$J_{\max} \equiv \min\big(J_{\max}^{\rm vib}, J_{\max}^{\rm rot}\big). \qquad (2.17)$$

For H_2, it results $J_{\max}^{\rm vib} = 43$ and $J_{\max}^{\rm rot} = 24$, so that $J_{\max} = 24$ and the cutoff curve has actually two parts. The two curves may intersect for j^* solution of

$$j^*(j^*+1) = \frac{2}{\chi_e^2\kappa^4}\,\frac{\kappa^2 - \kappa + \frac13}{(\kappa - \frac13)(5 - 3\kappa)}. \qquad (2.18)$$

For H_2, the solution is found to be $j^* = 16$ and $n^* = 14$.

The first (lower) part is due to stationarity with respect to vibrations while the second (upper) part is due to stationarity with respect to rotations. Thus, the cutoff value N_j for any admissible rotational mode j of the H_2 molecule described to the Harris–Bertolucci spectrum will be defined by

$$N_j = \begin{cases} N^{\rm vib}(j) & \text{for } 0 \le j \le j^* \\ N^{\rm rot}(j) & \text{for } j^* \le j \le J_{\max} \end{cases} \qquad (2.19)$$

and gives a total of 342 states.[1] The function $z_{\rm rv}^{\rm HB}(T)$ is the dotted curve in Figure 1, with the values of the Morse parameters of H_2 given in Tables 1 and 2. The curve is found to provide a fairly good approximation of $z_{\rm rv}(T)$ that is based on the accurate numerical energy levels of Pachucki and Komasa [13]. Admittedly, near the cutoff the Harris–Bertolucci energy levels are of decreasing precision, but the accuracy of the remaining admissible states is such that an overall fairly good representation of the partition

[1] The combined rotational–vibrational character of the cutoff (2.19) is a distinctive feature of the Harris–Bertolucci spectrum of the molecular hydrogen H_2, a peculiarity shared only by the other two lightest diatomic molecules LiH, with $j^* = 39$ & $n^* = 20$, and Li_2, with $j^* = 106$ & $n^* = 37$. For any other diatomic molecule, the cutoff of the Harris–Bertolucci spectrum is merely vibrational.

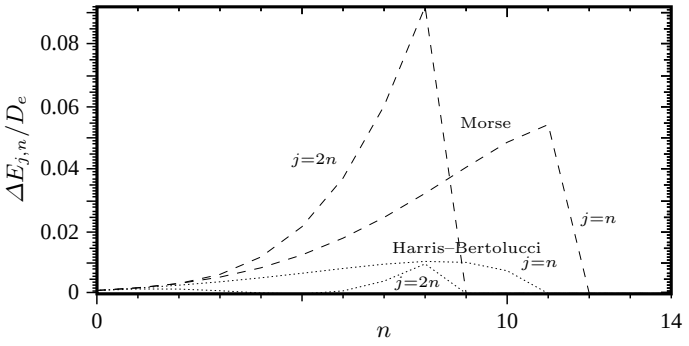

Fig. 2. Dimensionless energy difference $\Delta E_{j,n}/D_e$ between the Pachucki–Komasa numerical energy levels $E_{j,n}$ and the Harris–Bertolucci levels $E^{\text{HB}}_{j,n}$ of equation (2.12) (dotted curves) or the Morse levels $E^{\text{M}}_{j,n}$ of equation (2.20) (dashed curves), along two representative straight lines $j = n$ and $j = 2n$.

function is achieved for temperatures which are not too large. This quite positive behaviour is not shared by the spectrum of the Morse rotating oscillator [5, p. 64]. Using our parametrization χ_e-κ, the original Morse spectrum assumes the same expression (2.12) of Harris–Bartolucci except for the coefficient of the coupling term $j(j+1)\big(n+\frac{1}{2}\big)$, which is replaced as follows

$$-3(1-\kappa)(\kappa\chi_e)^3 \quad \to \quad -(\kappa\chi_e)^2\chi_e. \tag{2.20}$$

In this case the conditions $\partial E^{\text{M}}_{j,n}/\partial n = 0$ and $\partial E^{\text{M}}_{j,n}/\partial j = 0$ give relations $N^{\text{M}}_{\text{vib}}(j)$ and $N^{\text{M}}_{\text{rot}}(j)$ similar to those in (2.16), but with always $N^{\text{M}}_{\text{vib}}(j) > N^{\text{M}}_{\text{rot}}(j)$ and moreover $N^{\text{M}}_{\text{vib}}(0) = N^{\text{M}}_{\text{rot}}(0)$. Then, the cutoff for the Morse approximate spectrum can be based on either bounds $N^{\text{M}}_{\text{vib}}(j)$ or $N^{\text{M}}_{\text{rot}}(j)$, but in both cases the corresponding partition function is the dashed curve reported in Figure 1. The difference with respect to the curve based on Pachucki and Komasa energy levels is much lager than for the Harris–Bertolucci levels.

The origin of this difference can be clarified by plotting in Figure 2 the energy difference in dimensionless form $\Delta E_{j,n}/D_e$ along two straight lines $j = n$ and $j = 2n$ between the Pachucki–Komasa numerical energy levels $E_{j,n}$, assumed as reference values, and the approximate analytical values of the Harris–Bertolucci spectrum (dotted curves) or the Morse spectrum (dashed curves). For not too small n, the error of Morse energy levels along the bisecting line $j = n$ is substantially larger than that of the Harris–Bertolucci levels. The energy difference is due to the respective terms coupling rotations and vibrations, according to (2.20). This difference increases further along the second straight line $j = 2n$, thus demonstrating that the representation of the interaction by Morse spectrum is indeed too crude. On the contrary, the closed-form approximate spectrum of Harris–Bartolucci (2.12) together with the cutoff criterion defined by (2.16)–(2.19) represents a viable and analytically convenient alternative to the use of the full set of accurate numerical energy levels of Pachucki and Komasa, at least for the limited scope of deriving thermodynamic properties. In all our calculations, the various thermodynamic equations of state evaluated starting from the roto-vibrational energy levels of Pachucki and Komasa have been found to be virtually indistinguishable from those derived from Harris and Bertolucci approximate analytical spectrum (2.12).

To compute thermodynamic properties, the first and second derivatives of $z_{\text{rv}}(t)$ are needed. They can be evaluated through the intermediate functions $x_{\text{rv}}(t) = t^2 z'_{\text{rv}}(t)$ and $y_{\text{rv}}(t) = t^2 x'_{\text{rv}}(t)$ defined by

$$\begin{bmatrix} x_{\text{rv}}(t) \\ y_{\text{rv}}(t) \end{bmatrix} = \sum_{j=0}^{J_{\max}} \Delta_j \sum_{n=0}^{N_j} \begin{bmatrix} \varepsilon_{j,n} \\ \varepsilon_{j,n}^2 \end{bmatrix} \mathrm{e}^{-\varepsilon_{j,n}/t}, \tag{2.21}$$

where $\varepsilon_{j,n} = (E_{j,n} + D_e)/kT_{\text{v}}$.

When the approximate spectrum in closed form of Harris and Bertolucci (2.12) is used, the derivatives can be evaluated more simply as follows. First, the function $z^{\text{HB}}_{\text{rv}}(t) \leftarrow z^{\text{HB}}_{\text{rv}}(T)$ of the dimensionless temperature $t = T/T_{\text{v}}$ is introduced, namely,

$$z^{\text{HB}}_{\text{rv}}(t) = \sum_{j=0}^{J_{\max}} \Delta_j \, \mathrm{e}^{-\tilde{b}_j/t} \sum_{n=0}^{N_j} \mathrm{e}^{-a_n^j/t}, \tag{2.22}$$

where $\tilde{b}_j = b_j T_{\text{r}}/T_{\text{v}}$. Then, we introduce three sets of functions of the dimensionless temperature

$$\begin{bmatrix} A_j(t) \\ B_j(t) \\ C_j(t) \end{bmatrix} \equiv \sum_{n=0}^{N_j} \begin{bmatrix} 1 \\ a_n^j \\ (a_n^j)^2 \end{bmatrix} \mathrm{e}^{-a_n^j/t}, \quad 0 \le j \le J_{\max}, \tag{2.23}$$

whose derivatives satisfy the simple relations $dA_j(t)/dt = B_j(t)/t^2$ and $dB_j(t)/dt = C_j(t)/t^2$. Then, in terms of the definitions (2.23), the partition function (2.22) and its derivatives, required to obtain thermodynamic relations, are easily calculated by the summation

$$\begin{bmatrix} z^{\text{HB}}_{\text{rv}}(t) \\ x^{\text{HB}}_{\text{rv}}(t) \\ y^{\text{HB}}_{\text{rv}}(t) \end{bmatrix} \equiv \sum_{j=0}^{J_{\max}} \begin{bmatrix} A_j(t) \\ \tilde{b}_j A_j(t) + B_j(t) \\ \tilde{b}_j^2 A_j(t) + 2\tilde{b}_j B_j(t) + C_j(t) \end{bmatrix} \Delta_j \, \mathrm{e}^{-\tilde{b}_j/t} \tag{2.24}$$

3 Dissociating hydrogen without ionization

For temperatures before the occurrence of ionization, say, $T < 5000\,\text{K}$, a simple thermodynamic model of the hydrogen gas is easily obtained by finding the equilibrium composition of the dissociating gas that minimizes the Helmholtz free energy, see, *e.g.* [12, p. 185]. Let $\mathcal{N}_{\text{H}_2}$ be the total number of H_2 molecules in the volume V when all molecules are undissociated. The degree of dissociation α of the gas in a state with N_{H_2} molecules is defined by

$$\alpha = \frac{\mathcal{N}_{\text{H}_2} - N_{\text{H}_2}}{\mathcal{N}_{\text{H}_2}}, \tag{3.1}$$

so that $N_{\text{H}_2} = (1-\alpha)\mathcal{N}_{\text{H}_2}$ and, thanks to the conservation of the total number of hydrogen nuclei, $2N_{\text{H}_2} + N_{\text{H}} =$

$\mathcal{N}_{\rm H} = 2\mathcal{N}_{\rm H_2}$, also $N_{\rm H} = 2\alpha\mathcal{N}_{\rm H_2} = \varsigma\alpha\mathcal{N}_{\rm H_2}$. Here, the constant ς is the symmetry factor of the molecule, $\varsigma = 2$ for homonuclear molecules and equal to 1 for heteronuclear molecules. By minimizing the free energy (2.1), we obtain the equation for dissociation equilibrium

$$\frac{N_{\rm H}^2}{N_{\rm H_2}} = \frac{[Z_{\rm H}(T,V)]^2}{Z_{\rm H_2}(T,V)}. \tag{3.2}$$

Expressing $N_{\rm H}$ and $N_{\rm H_2}$ in terms of α, the equation for the dissociation equilibrium becomes

$$\frac{\alpha^2}{1-\alpha} = \frac{K(T)}{\varsigma_{\rm H_2}^2}\,\frac{V}{\mathcal{N}_{\rm H_2}}, \tag{3.3}$$

where the equilibrium constant $K(T) = \frac{[Z_{\rm H}(T,V)/V]^2}{Z_{\rm H_2}(T,V)/V}$ using (2.7) and (2.8) with $E_{\rm H,0} = 0$ and $E_{\rm H_2,0} = 0$, is defined by

$$K(T) = C_{\rm d}\cdot\left(\frac{T}{T_{\rm v}}\right)^{\frac{3}{2}}\frac{{\rm e}^{-T_D/T}}{z_{\rm rv}(T/T_{\rm v})}, \tag{3.4}$$

where $T_D = D_e/k = 55\,121\,{\rm K}$ and

$$C_{\rm d} = \frac{(g_{\rm H}^{\rm n})^2}{2\sqrt{2}}\,\frac{(g_{\rm H}^{\rm el})^2}{g_{\rm H_2}^{\rm el}}\left(\frac{m_{\rm H}kT_{\rm v}}{2\pi\hbar^2}\right)^{\frac{3}{2}}. \tag{3.5}$$

The occurrence of the energy depth $D_e = kT_D$ in function $K(T)$ instead of the molecular dissociation energy of the Morse anharmonic oscillator, $U = -E_{j=0,\,n=0} = \big(1-\frac{\chi_e}{2}\big)^2 D_e$ ($U_{\rm H_2} = 4.483\,{\rm eV}$), is only apparent. In fact, the denominator $z_{\rm rv}(T/T_{\rm v})$ contains the following factor $\exp\big[-\frac{1}{2}\big(1-\frac{\chi_e}{4}\big)T_{\rm v}/T\big]$ that combines, with ${\rm e}^{-T_D/T}$, to give ${\rm e}^{-T_U/T}$, with $T_U = U/k$.

In terms of the dimensionless temperature $t = T/T_{\rm v}$ and of the specific volume $v = V/(m_{\rm H_2}\mathcal{N}_{\rm H_2})$, the equation for the dissociation equilibrium reads

$$\frac{\alpha^2}{1-\alpha} = \frac{t^{\frac{3}{2}}\,{\rm e}^{-t_D/t}}{z_{\rm rv}(t)}\,\frac{v}{\varsigma_{\rm H_2}^2\,\bar v_{\rm d}}, \tag{3.6}$$

where $t_D = T_D/T_{\rm v} = D_e/kT_{\rm v} = 8.749$ and with the scale constant $v_{\rm d}$ for the variable v defined by

$$\bar v_{\rm d}^{-1} = m_{\rm H_2}C_{\rm d}. \tag{3.7}$$

Being $g_{\rm H}^{\rm el} = 2$ and $g_{\rm H_2}^{\rm el} = 1$ for the molecular ground state ${}^1\Sigma_g^+$, we have $\bar v_{\rm d}^{-1} = 1.7655\times10^6\,{\rm kg/m^3}$ and $\bar v_{\rm d} = 0.56641\times10^{-6}\,{\rm m^3/kg}$.

The energy E of the hydrogen gas model is obtained from $F(T,V,N_{\rm H_2},N_{\rm H})$ by means of the relation $E = F - T(\partial F/\partial T)_{V,N_{\rm H_2},N_{\rm H}}$, which yields the dimensionless specific energy $\epsilon = e/R_{\rm H_2}T_{\rm v}$ (with $e = E/m_{\rm H_2}\mathcal{N}_{\rm H_2}$ and $R_{\rm H_2} = 4157.2\,{\rm J/(kg\cdot K)}$),

$$\epsilon(t,\alpha) = \tfrac{3}{2}(1+\alpha)\,t + (1-\alpha)[\epsilon_{\rm rv}(t) - t_D], \tag{3.8}$$

where

$$\epsilon_{\rm rv}(t) = \frac{x_{\rm rv}(t)}{z_{\rm rv}(t)}. \tag{3.9}$$

At zero temperature $\epsilon(0,0) = \epsilon_{\rm rv}(0) - t_D$. It is common to normalize the energy by adding the energy depth D_e of the Morse potential so that the energy for $T\to0$ is positive and includes the zero point energy shift $\hbar\omega_e/2$, namely $\tilde\epsilon(t,\alpha) = \epsilon(t,\alpha) + t_D$. The final expression of the new normalized energy, denoted by the same letter ϵ for notational simplicity, will be

$$\epsilon(t,\alpha) = \tfrac{3}{2}(1+\alpha)\,t + (1-\alpha)\,\epsilon_{\rm rv}(t) + \alpha t_D, \tag{3.10}$$

and now $\epsilon(0,0) = \epsilon_{\rm rv}(0)$, as required.

Relation (3.10) for the internal energy must be compared with the analogous expression obtained by considering the mixture of ideal gases and summing directly the energy of the molecular and atomic components. Assuming that all energy contributions due to the electronic excitation can be neglected, the dimensionless expression of the energy of the ideal gas mixture with fully classical rotations and vibrations may be represented in the form, see, *e.g.*, Capitelli, Colonna e D'Angola [20, p. 19],

$$\begin{aligned}\epsilon^{\rm mix}(t,\alpha) &= \tfrac{1}{2}(7-\alpha)\,t + \alpha t_U\\ &= \tfrac{3}{2}(1+\alpha)\,t + 2(1-\alpha)\,t + \alpha t_U,\end{aligned} \tag{3.11}$$

where $t_U = U/kT_{\rm v}$. By including the zero-point energy shift and using $t_D - t_U = \frac{1}{2}\big(1-\frac{\chi_e}{4}\big) \approx \frac{1}{2}$, we have

$$\tfrac{1}{2} + \epsilon^{\rm mix}(t,\alpha) = \tfrac{3}{2}(1+\alpha)\,t + (1-\alpha)\big(\tfrac{1}{2}+2t\big) + \alpha t_D, \tag{3.12}$$

to be compared with relation (3.10). Thus, the term that should be compared with $\epsilon_{\rm rv}(t)$ is simply $\frac{1}{2}+2t$. The functions $\epsilon_{\rm rv}(t)$ and $\frac{1}{2}+2t$ are represented in Figure 3 by the continuous and dot-dashed curves, respectively.

The straight line $2t$ of the ideal gas mixture reflects the assumption of fully classical rotations and vibrations. For completeness, in the same figure we plot also the curves of two other possible approximations for the molecular energy of H_2: the dashed curve corresponds to the molecular energy $t + \epsilon_{\rm v}(t)$ consisting of fully excited rotations but quantum vibrations according to the Morse anharmonic oscillator (detailed in Section 7); and finally the dotted curve is the molecular energy $t + \epsilon_{\rm v}^{\rm har}(t) = t + \frac{1}{2} + \frac{{\rm e}^{-1/t}}{1-{\rm e}^{-1/t}}$ for fully excited classical rotations and the Einstein quantum linear oscillator.

The slope of the curves in Figure 3 at large temperatures is related to the finite or infinite number of quantum states of the molecule: the roto-vibrational model represented by the continuous curve $\epsilon_{\rm rv}(t)$ has a finite number of states, leading to a zero slope; the Morse simpler model with $\epsilon_{\rm v}(t)$ has a finite number of vibrational states but an infinite number of rotational states, implying a curve with slope 1, asymptotically; in the other two models (Einstein quantum oscillator and the ideal gas mixture) both rotational and vibrational states are infinite and the slope of the curve is 2 as $t\to\infty$ and for any t, in the two cases. The great differences in the molecular energy in the range $t > 2$ and for a density not exceeding $\rho \sim 10\,{\rm kg/m^3}$ are however not important because in this range of temperatures the dissociation is complete and the contribution to

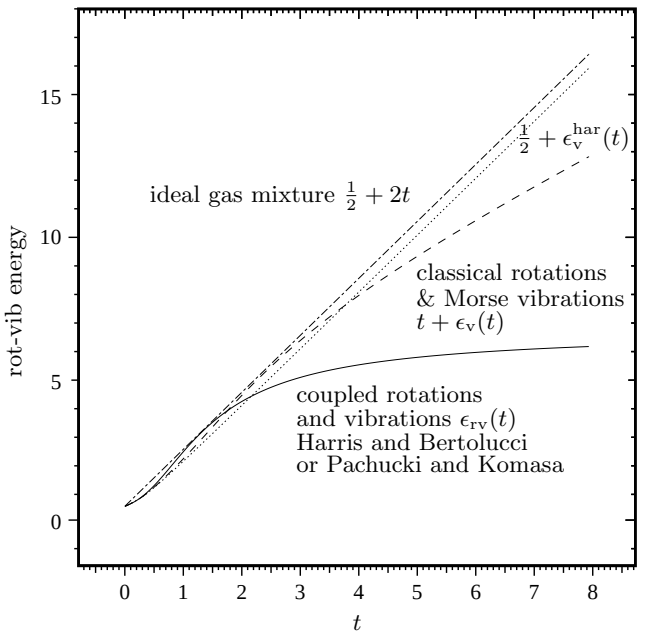

Fig. 3. Dimensionless roto-vibrational energy of the H_2 molecule as a function of the dimensionless temperature $t = T/T_{\rm v}$. Continuous curve: molecular energy $\epsilon_{\rm rv}(t)$ of the rotating oscillator with Harris–Bertolucci or Pachucki–Komasa spectrm. In the remaining three curves, the rotations are accounted for classically as fully excited. Dashed curve: $t+\epsilon_{\rm v}(t)$ with molecular vibrations described by the nonrotating Morse anharmonic oscillator. Dotted curve: $t+\epsilon_{\rm v}^{\rm har}(t)$ with harmonic molecular vibrations. Dot-dashed curve: function $\frac{1}{2}+2t$ which is the *internal* energy contribution of H_2 plus the point energy, cf. equation (3.12).

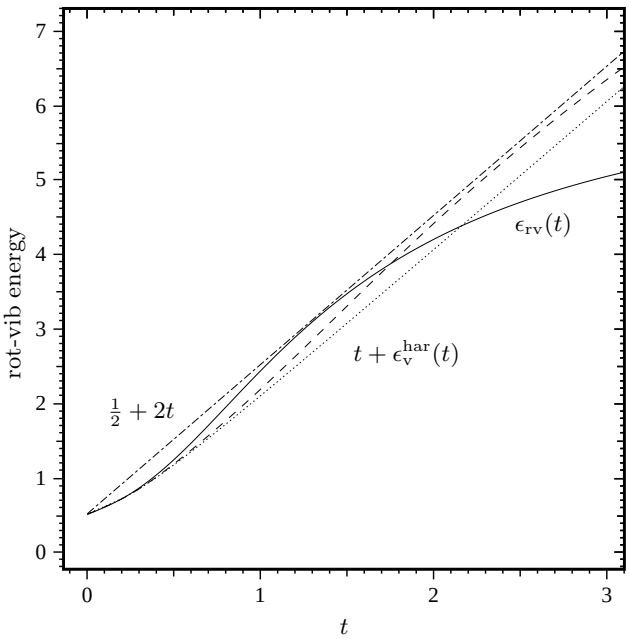

Fig. 4. Particular of Figure 3 representing the dimensionless roto-vibrational energy of the H_2 molecule. The same labeling for the curves used in the previous figure applies here. The dotted curve corresponds to the model with fully excited classical rotations combined with the harmonic molecular vibrations of the Einstein quantum oscillator, namely, $t+\epsilon_{\rm v}^{\rm har}(t)$.

the energy of this term vanishes. For lower temperatures, in the range of only partial dissociation, the differences are much smaller and they are displayed more clearly in Figure 4 which contains an enlargement of the bottom-left corner of Figure 3. The initial unit slope of the curves of three models corresponds to the rotational contribution t to the energy which is built inside the function $\epsilon_{\rm rv}(t)$ or is included explicitly in both the nonharmonic (nonrotating Morse) and harmonic models. The comparison of the different energies for not too large temperatures reveals that the fully classical approximation of the ideal gas mixture is a fairly good approximation of the Einstein oscillator model except for rather small t. Moreover, the gas mixture model gives an acceptable approximation of the energy, with differences becoming appreciably large only for $t > 2$. The description of the molecular energy provided by the roto-vibrating model $\epsilon_{\rm rv}(t)$ is in general more satisfactory than the other models. The real interest of this physically more complete model is due to the possibility of building a corresponding term for the entropy equation, as it will be described below. In this way, two fully compatible equations of state for energy and entropy can be built so as to guarantee a complete representation of the fundamental thermodynamic relation of the gas system. In Figure 5 the internal energy $e(T, v)$ of the present model (continuous curves) is compared with the function (3.12) of the ideal gas mixture model (dot-dashed curves) for the specific volume values $v = 10^{\ell}\ {\rm m}^3/{\rm kg}$, for $\ell = -1, 0, 1, 2, 3$. In the range of dissociation temperatures the two models agree fairly well except for small differences at the lower tempertaures due to the straight line approximation of the vibrational energy. The differences at the higher temperatures of the plot are instead due only to the fact that the continuous curves refer to a thermodynamic model including the possibility of ionization (see below) which is not accounted in the ideal gas mixture approximation (3.12).

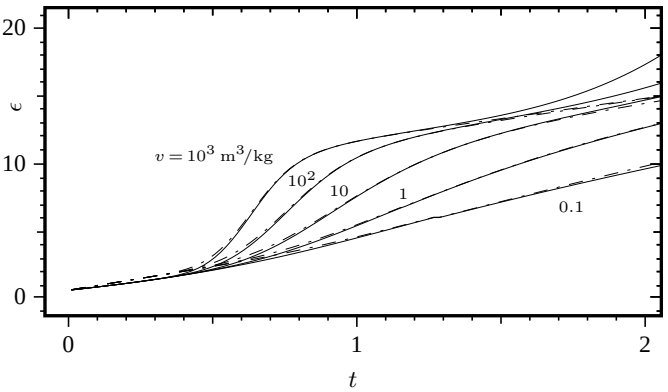

Fig. 5. Dimensionless internal energy ϵ in the range of dissociation temperatures for different values of v. Comparison of the present thermodynamic model (continuous curve) with the ideal gas mixture model of equation (3.12) (dot-dashed curve).

Similarly to the energy, the dimensionless specific entropy $\sigma = s/R_{\mathrm{H}_2} = S/m_{\mathrm{H}_2}\mathcal{N}_{\mathrm{H}_2}/R_{\mathrm{H}_2} = S/(m_{\mathrm{H}_2}R_{\mathrm{H}_2}\mathcal{N}_{\mathrm{H}_2})$ is obtained from F by $S = -(\partial F/\partial T)_{V,N_{\mathrm{H}_2},N_{\mathrm{H}}}$, to give

$$\sigma(t,v,\alpha) = (1+\alpha)\left[\frac{5}{2} + \frac{3}{2}\,\ln t + \ln\left(\frac{v}{\bar{v}_{\mathrm{d}}}\right)\right] + (1-\alpha)\,\sigma_{\mathrm{rv}}(t) + \Upsilon_\varsigma(\alpha) + \sigma_0^{\mathrm{i}=0}, \tag{3.13}$$

where, cf. *e.g.*, [21],

$$\sigma_{\mathrm{rv}}(t) = \ln z_{\mathrm{rv}}(t) + \frac{x_{\mathrm{rv}}(t)}{t z_{\mathrm{rv}}(t)}, \tag{3.14}$$

and

$$\Upsilon_\varsigma(\alpha) = -(1-\alpha)\ln(1-\alpha) - 2\alpha\ln(\varsigma\alpha). \tag{3.15}$$

The function $\sigma_{\mathrm{rv}}(t)$ represents the contribution of the rotational-vibrational entropy of the molecule while function $\Upsilon_\varsigma(\alpha)$ is the entropy of the mixing of the molecular and atomic species. Finally $\sigma_0^{\mathrm{i}=0}$ is an arbitrary constant. The presence of the contribution $(1-\alpha)\sigma_{\mathrm{rv}}(t)$ in the entropy ensures the compatibility with the term $(1-\alpha)\epsilon_{\mathrm{rv}}(t)$ of the energy, similarly to nondissociating molecular ideal gases with variable specific heats, see, e.g., in [22, p. 33]. In this case, the full compatibility is guaranteed by the fact that the roto-vibrational contribution $(1-\alpha)\sigma_{\mathrm{rv}}(t)$ to the entropy occurs together with the mixing entropy function $\Upsilon_\varsigma(\alpha)$. The leading part of entropy relation (3.13) is akin to the Sackur–Tetrode equation for monatomic gas [23] but (3.13) applies to a roto-vibrating diatomic gas, with the dissociation α fixed by the equilibrum condition (3.6). The solution to the latter, namely,

$$\alpha(t,v) = \tfrac{1}{2}\mathcal{D}^0(t,v)\big[\sqrt{1+4/\mathcal{D}^0(t,v)}\,-1\big], \tag{3.16}$$

with $\mathcal{D}^0(t,v) = \frac{t^{\frac{3}{2}}\,\mathrm{e}^{-t_D/t}}{z_{\mathrm{rv}}(t)}\,\frac{v}{\varsigma^2 v_{\mathrm{d}}}$, is substituted into (3.10) and (3.13) to obtain eventually the equations of state of energy and entropy

$$e(T,v) = R_{\mathrm{H}_2}T_{\mathrm{v}}\,\epsilon\big(T/T_{\mathrm{v}}, \alpha(T/T_{\mathrm{v}},v)\big) \quad \text{and} \tag{3.17}$$

$$s(T,v) = R_{\mathrm{H}_2}\,\sigma\big(T/T_{\mathrm{v}}, v, \alpha(T/T_{\mathrm{v}},v)\big), \tag{3.18}$$

both being functions only of T and v. The two functions provide a compatible parametric representation of the fundamental thermodynamic relation $s = s(e,v)$ or $e = e(s,v)$ of the roto-vibra-dissociating hydrogen gas. The parametric form is strictly equivalent to the original fundamental relation (2.1) of the free energy $F(T,V,N_{\mathrm{H}_2},N_{\mathrm{H}})$, we have started from. But the availability of the two explicit functions $e(T,v)$ and $s(T,v)$ is very useful in fluid dynamics applications, where the energy and entropy relations are required to describe, for instance, adiabatic irreversible transformations produced by shock waves and isentropic processes occurring in rarefaction waves. On the other hand, for temperatures $T > 5000\,\mathrm{K}$ hydrogen atoms can ionize and the effects of ionization cannot be neglected anymore. A possible manner of including the atomic ionization effects in a thermodynamic description of the hydrogen gas is proposed in the following.

4 Dissociation and ionization at equilibrium

The model for the ionizable hydrogen gas proposed here assumes that the gas is a mixture of molecular hydrogen H_2, atomic hydrogen H as well as free protons and electrons, resulting from the ionization of the neutral atoms. The chemical model underlying the system consists in the dissociation and ionization reactions

$$\mathrm{H}_2 \;\rightleftharpoons\; 2\mathrm{H} \qquad \text{and} \qquad \mathrm{H} \;\rightleftharpoons\; \mathrm{p} + \mathrm{e}. \tag{4.1}$$

The mixture comprises therefore the two chemical species, H_2 and H, together with bare protons and electrons, p and e. Thus, the model excludes the possibility of the processes of molecular ionization, $\mathrm{H}_2 \rightleftharpoons \mathrm{H}_2^+ + \mathrm{e}$ and of formation of negatively charged hydrogenic ions, $\mathrm{H}_2 \rightleftharpoons \mathrm{H}^- + \mathrm{p}$. As shown by Alastuey and Ballenegger [11], the reactions forming the ions H_2^+ and H^- can be neglected.

In a given generic thermodynamic state of the gas there are N_{H_2} molecules of H_2, together with N_{H} neutral hydrogen atoms and N_{p} protons and $N_{\mathrm{e}} = N_{\mathrm{p}}$ electrons, due to the overall charge neutrality of the gas. The degree of dissociation of the molecular hydrogen and the dgree of atomic ionization are measured by the dissociation and ionization coefficients

$$\alpha = \frac{\mathcal{N}_{\mathrm{H}_2} - N_{\mathrm{H}_2}}{\mathcal{N}_{\mathrm{H}_2}} \qquad \text{and} \qquad i = \frac{N_{\mathrm{p}}}{2\alpha\mathcal{N}_{\mathrm{H}_2}}. \tag{4.2}$$

Thanks to the conservation of the total number of hydrogen nuclei, $2N_{\mathrm{H}_2} + N_{\mathrm{H}} + N_{\mathrm{p}} = \mathcal{N}_{\mathrm{H}} = 2\mathcal{N}_{\mathrm{H}_2}$, and to the charge neutrality, $N_{\mathrm{p}} = N_{\mathrm{e}}$, the mole numbers of the gas components are easily found in terms of $\mathcal{N}_{\mathrm{H}_2}$

$$\begin{aligned} N_{\mathrm{H}_2}(\alpha) &= (1-\alpha)\mathcal{N}_{\mathrm{H}_2},\\ N_{\mathrm{H}}(\alpha,i) &= 2\alpha(1-i)\mathcal{N}_{\mathrm{H}_2},\\ N_{\mathrm{p}}(\alpha,i) &= 2\alpha i\mathcal{N}_{\mathrm{H}_2}. \end{aligned} \tag{4.3}$$

The total number of moles is $N(\alpha,i) = (1+\alpha+2\alpha i)\mathcal{N}_{\mathrm{H}_2}$ and the molar fractions are

$$\begin{aligned} X_{\mathrm{H}_2}(\alpha,i) &\equiv \frac{N_{\mathrm{H}_2}(\alpha)}{N(\alpha,i)} = \frac{1-\alpha}{1+\alpha+2\alpha i},\\ X_{\mathrm{H}}(\alpha,i) &\equiv \frac{N_{\mathrm{H}}(\alpha,i)}{N(\alpha,i)} = \frac{2\alpha(1-i)}{1+\alpha+2\alpha i},\\ X_{\mathrm{p}}(\alpha,i) &\equiv \frac{N_{\mathrm{p}}(\alpha,i)}{N(\alpha,i)} = \frac{2\alpha i}{1+\alpha+2\alpha i}. \end{aligned} \tag{4.4}$$

The free energy of the system of noninteracting particles comprising the four species H_2, H, p and e is given by

$$F = -kT\ln\left(\frac{Z_{\mathrm{H}_2}^{N_{\mathrm{H}_2}}}{N_{\mathrm{H}_2}!}\,\frac{Z_{\mathrm{H}}^{N_{\mathrm{H}}}}{N_{\mathrm{H}}!}\,\frac{Z_{\mathrm{p}}^{N_{\mathrm{p}}}}{N_{\mathrm{p}}!}\,\frac{Z_{\mathrm{e}}^{N_{\mathrm{e}}}}{N_{\mathrm{e}}!}\right), \tag{4.5}$$

where $Z_{\mathrm{H}_2} = Z_{\mathrm{H}_2}(T,V)$, $Z_{\mathrm{H}} = Z_{\mathrm{H}}(T,V)$, $Z_{\mathrm{p}} = Z_{\mathrm{p}}(T,V)$ and $Z_{\mathrm{e}} = Z_{\mathrm{e}}(T,V)$ are the partition functions of H_2, H, p and e, respectively. The assumption underlying this Helmholtz potential is that any interaction between all

particles can be neglected completely, as in an ideal gas mixture. The assumption was acceptable at low densities for the dissociating hydrogen gas without ionization with free energy (2.1), but is always violated for a ionized gas, due to the electrostatic interaction between the charged particles. However, when the gas density is such that the Coulomb interaction energy between neighboring charges is small with respect to their kinetic energy, the ionized gas can be considered as only weakly noindeal and the Helmholtz free energy (4.5) for noninteracting particles can be assumed as the starting point, see, *e.g.*, [12, p. 215]. For example, in the hydrogen gas of interest here, with an atomic density $\widetilde{N}$ and an average distance between the particles $\langle r\rangle \approx \widetilde{N}^{-1/3}$, the condition for an ideal behavior is $\widetilde{N} < \left(\frac{kT}{q_{\rm e}^2/4\pi\epsilon_0}\right)^3$ which at $T = 30000\,\mathrm{K}$ gives for the specific volume the condition $v > 0.1\,\mathrm{m}^3/\mathrm{kg}$. For higher densities, corrections accounting for Coulomb interaction are necessary, but their consideration and inclusion are beyond the scope of this work.

The stationarity of the free energy (4.5) with respect to dissociation and ionization gives the two equations

$$\frac{N_{\rm H}^2}{N_{\rm H_2}} = \frac{Z_{\rm H}^2(T,V)}{Z_{\rm H_2}(T,V)}, \tag{4.6}$$

$$\frac{N_{\rm p}^2}{N_{\rm H}} = \frac{Z_{\rm p}(T,V)\,Z_{\rm e}(T,V)}{Z_{\rm H}(T,V)}. \tag{4.7}$$

Using the expressions of $N_{\rm H_2}, N_{\rm H}$ and $N_{\rm p}$ in (4.3), the two relations give the following system of algebraic equations

$$\begin{cases} \alpha^2(1-i)^2 = D(T,V,\mathcal{N}_{\rm H_2})(1-\alpha), \\ \alpha i^2 = I(T,V,\mathcal{N}_{\rm H_2})(1-i), \end{cases} \tag{4.8}$$

where

$$D(T,V,\mathcal{N}_{\rm H_2}) \equiv \frac{[Z_{\rm H}(T,V)]^2}{4Z_{\rm H_2}(T,V)}\,\frac{1}{\mathcal{N}_{\rm H_2}}, \tag{4.9}$$

$$I(T,V,\mathcal{N}_{\rm H_2}) \equiv \frac{Z_{\rm p}(T,V)\,Z_{\rm e}(T,V)}{2Z_{\rm H}(T,V)}\,\frac{1}{\mathcal{N}_{\rm H_2}}. \tag{4.10}$$

The partition function for the hydrogen molecule is as discussed so far, namely,

$$Z_{\rm H_2}(T,V) = \left(\frac{m_{\rm H_2}kT}{2\pi\hbar^2}\right)^{\frac{3}{2}} z_{\rm rv}(T/T_{\rm v}) \times g_{\rm H_2}^{\rm el}\,\mathrm{e}^{(D_{\rm e}-E_{\rm H_2,0})/kT}\,V. \tag{4.11}$$

The partition function of the hydrogen atom is taken in the form

$$Z_{\rm H}(T,V) = Z_{\rm H}^{\rm tr}(T,V)\,Z_{\rm H}^{\rm nuc,el}(T) = \left(\frac{m_{\rm H}kT}{2\pi\hbar^2}\right)^{\frac{3}{2}} g_{\rm H}^{\rm n}\,Z_{\rm H}^{\rm el}(T)\,V. \tag{4.12}$$

The electronic partition function $Z_{\rm H}^{\rm el}(T)$ must include the energy levels of the electron in the excited bound quantum states[2] of the hydrogen atom, namely, the energy values

$$E_n = -\frac{I_{\rm H}}{n^2}, \qquad n = 1, 2, \ldots \tag{4.13}$$

where $I_{\rm H} = \frac{m_{\rm e}q_{\rm e}^4}{8h^2\epsilon_0^2} = 13.60\,\mathrm{eV}$ denotes the ionization energy of the hydrogen. However, the partition function

$$Z_{\rm H}^{\rm el}(T) = g_{\rm H}^{\rm el}\sum_{n=1}^{\infty} n^2\,\mathrm{e}^{-E_n/kT} = g_{\rm H}^{\rm el}\sum_{n=1}^{\infty} n^2\,\mathrm{e}^{T_{\rm i}/n^2T}, \tag{4.14}$$

with $T_{\rm i} = I_{\rm H}/k = 157\,800\,\mathrm{K}$, cannot be used directly since the series is divergent. To circumvent this obstacle, a method originally introduced by Fermi is adopted [15]. The rule of Fermi consists in assigning an *a priori* probability of the quantum state, decreasing with the volume of the excited atom and *depending* on the gas density, to give

$$Z_{\rm H}^{\rm el}(T,v) = g_{\rm H}^{\rm el}\sum_{n=1}^{\infty} n^2\,\mathrm{e}^{T_{\rm i}/n^2T}\mathrm{e}^{-4B\hat{N}(v)\,n^6} = g_{\rm H}^{\rm el}\,\mathrm{e}^{T_{\rm i}/T}\sum_{n=1}^{\infty} n^2\,\mathrm{e}^{-\left(1-\frac{1}{n^2}\right)\frac{T_{\rm i}}{T}\,-\,4B\hat{N}(v)\,n^6}, \tag{4.15}$$

where $B = \frac{4}{3}\pi a_0^3$, $a_0 = \frac{4\pi\epsilon_0\hbar^2}{m_{\rm e}q_{\rm e}^2} = 5.29\times10^{-11}\,\mathrm{m}$ is the Bohr radius, and $\hat{N}(v) = 1/(vm_{\rm H})$ is the density of hydrogen nuclei. Thus, the definition $Z_{\rm H}^{\rm el}(T,v) = g_{\rm H}^{\rm el}\,\mathrm{e}^{T_{\rm i}/T}z_{\rm H}(\tau,v)$, allow us to introduce the atomic partition function, dependent both on the dimensionless temperature $\tau = T/T_{\rm i}$,

$$z_{\rm H}(\tau,v) = \sum_{n=1}^{\infty} n^2\,\mathrm{e}^{-\left(1-\frac{1}{n^2}\right)\frac{1}{\tau}\,-\,4B\hat{N}(v)\,n^6}, \tag{4.16}$$

and on the specific volume v, due to the presence of $\hat{N}(v)$ in the Fermi cutoff (as in other similar rules, see below). The Fermi cutoff is a form of the occupation probability methods, that are used to have a finite internal partition function $z_{\rm H}$, in the study of dense plasmas, see, *e.g.*, [8]. In these applications the numbers N_n of atoms in the electronically excited state E_n are retained as independent thermodynamic variables. Some criticisms are presently raised concerning the consistency of some expressions of the free energy used by the occupation probability methods [24]–[26]. These criticisms do not apply to the present derivation since our thermodynamic model is limited to diluted conditions and, above all, has a single variable $N_{\rm H}$ to describe the total number of all neutral atoms, irrespective of their state of electronic excitation. Stated in other terms, the Fermi cutoff is used here not to represent the occupancy of the excited level, but only to reduce them to a finite number, so as to make a path toward the production of pairs of (noninteracting) charges available, much in the same manner of the molecular dissociation mechanism.

[2] In this section, n denotes the principal quantum number of the atomic electron state, and is not the quantum number of the molecular vibrations, as elsewhere in the paper.

Alternatively, according to Zel'dovich [12, p. 199] an even simpler manner to avoid the divergence is to truncate the sum by retaining only the electron states before the size of the electronically excited atom is large enough to interfere with the neighboring atoms at the considered gas density. This leads to the truncated series, with $\tau = T/T_{\rm i}$,

$$z_{\rm H}^{\rm cutoff}(\tau, v) = \sum_{n=1}^{n_{\rm cutoff}(v)} n^2 \, {\rm e}^{-\left(1-\frac{1}{n^2}\right)\frac{1}{\tau}}, \tag{4.17}$$

where

$$n_{\rm cutoff}(v) = \frac{1}{2}\Big(\frac{m_{\rm H} v}{a_0^3}\Big)^{\frac{1}{6}} \qquad (n_{\rm cutoff} \geq 1). \tag{4.18}$$

Thus, the complete partition function for the hydrogen atom for modelling the gas/plasma is assumed to be

$$Z_{\rm H}(T, V) = \left(\frac{m_{\rm H} kT}{2\pi\hbar^2}\right)^{\frac{3}{2}} g_{\rm H}^{\rm n} \, g_{\rm H}^{\rm el} \, {\rm e}^{I_{\rm H}/kT} \, z_{\rm H}(T/T_{\rm i}, v) \, V. \tag{4.19}$$

Finally, the partition functions for the free proton and electron are

$$Z_{\rm p}(T, V) = 2\left(\frac{m_{\rm p} kT}{2\pi\hbar^2}\right)^{\frac{3}{2}} {\rm e}^{-E_{\rm p,0}/kT} \, V, \tag{4.20}$$

$$Z_{\rm e}(T, V) = 2\left(\frac{m_{\rm e} kT}{2\pi\hbar^2}\right)^{\frac{3}{2}} {\rm e}^{-E_{\rm e,0}/kT} \, V, \tag{4.21}$$

where the 2's are due to the spin $\frac{1}{2}$ of proton and electron.

By taking $E_{\rm H_2,0} = -2I_{\rm H}$ and $E_{\rm p,0} = E_{\rm e,0} = 0$, the equilibrium constants of dissociation and ionization are respectively

$$K_{\rm d}(T, v) = C_{\rm d} \cdot \left(\frac{T}{T_{\rm v}}\right)^{\frac{3}{2}} {\rm e}^{-T_D/T} \, \frac{[z_{\rm H}(T/T_{\rm i}, v)]^2}{z_{\rm rv}(T/T_{\rm v})}, \tag{4.22}$$

$$K_{\rm i}(T, v) = C_{\rm i} \cdot \left(\frac{T}{T_{\rm i}}\right)^{\frac{3}{2}} \frac{{\rm e}^{-T_{\rm i}/T}}{z_{\rm H}(T/T_{\rm i}, v)}, \tag{4.23}$$

with the constant $C_{\rm d}$ is defined in (3.5) while

$$C_{\rm i} = \frac{2}{g_{\rm H}^{\rm n} \, g_{\rm H}^{\rm el}} \left(\frac{m_{\rm p} m_{\rm e} kT_{\rm i}}{2\pi m_{\rm H} \hbar^2}\right)^{\frac{3}{2}}. \tag{4.24}$$

Using the partition functions (4.11), (4.19), (4.20) and (4.21) the system of the equilibrium equations is recast in the form

$$\begin{cases} \alpha^2 (1-i)^2 = \mathcal{D}(t, v)(1-\alpha), \\ \alpha i^2 = \mathcal{I}(t, v)(1-i), \end{cases} \tag{4.25}$$

with the functions $\mathcal{D} = \frac{1}{4} m_{\rm H_2} K_{\rm d} v/v_{\rm d}$ and $\mathcal{I} = m_{\rm H_2} K_{\rm i} v/v_{\rm i}$ controlling the coupled dissociation and ionization equilibria defined by

$$\mathcal{D}(t, v) = t^{\frac{3}{2}} \, {\rm e}^{-t_D/t} \, \frac{[z_{\rm H}(t/t_{\rm i}, v)]^2}{z_{\rm rv}(t)} \, \frac{v}{v_{\rm d}}, \tag{4.26}$$

$$\mathcal{I}(t, v) = \left(\frac{t}{t_{\rm i}}\right)^{\frac{3}{2}} \frac{{\rm e}^{-t_{\rm i}/t}}{z_{\rm H}(t/t_{\rm i}, v)} \, \frac{v}{v_{\rm i}}, \tag{4.27}$$

where $t_D = T_D/T_{\rm v} = D_e/kT_{\rm v}$, $t_{\rm i} = T_{\rm i}/T_{\rm v} = I_{\rm H}/kT_{\rm v}$ and

$$v_{\rm d}^{-1} = \frac{m_{\rm H_2} C_{\rm d}}{4} \quad \text{and} \quad v_{\rm i}^{-1} = m_{\rm H_2} C_{\rm i}. \tag{4.28}$$

The calculation yields $v_{\rm d} = 2.26564 \times 10^{-6}\,{\rm m^3/kg}$ and $v_{\rm i} = 4.02157 \times 10^{-3}\,{\rm m^3/kg}$.

The two equilibrium equations (4.25) are both quadratic, the first both in α and i, while the second only in i. The system reduces to a single fourth order algebraic equation

$$i^4 + ai^3 + bi^2 + ci + d = 0 \tag{4.29}$$

with the four coefficients a, b, c, d defined in terms of $\mathcal{D}(t, v)$ and $\mathcal{I}(t, v)$:

$$\begin{aligned} a &= \frac{(\mathcal{D} + 4\mathcal{I})\mathcal{I}}{\mathcal{D} - \mathcal{I}^2}, \qquad & b &= -\frac{(\mathcal{D} + 6\mathcal{I})\mathcal{I}}{\mathcal{D} - \mathcal{I}^2}, \\ c &= \frac{4\mathcal{I}^2}{\mathcal{D} - \mathcal{I}^2}, & d &= -\frac{\mathcal{I}^2}{\mathcal{D} - \mathcal{I}^2}. \end{aligned} \tag{4.30}$$

For all values $v > 10^{-5}\,{\rm m^3/kg}$ and $T < 10^6\,{\rm K}$ this equation has been found to possess only one real root in the unit interval $[0, 1]$; for higher temperatures, a solution i extremely near to 1 is easily selected as the proper one among three real admissible values. The dissociation α is given by $\alpha = \mathcal{I}(1-i)/i^2$.

A fourth-order equation for the electron partial pressure $P_{\rm e}$ is considered in Capitelli's monograph [20], whose coefficients are defined in terms of the equilibrium constants for dissociation and ionization. When they are known as a function of T, the gas total pressure P can be determined and subsequently also α and i. Actually, the equilibrium constants are function of two thermodynamic variables, and therefore the problem for the partial pressure is nonlinear, beyond the algebraic quartic character. However, in practice the dependence of the solution on the second thermodynamic variable v is rather weak and a couple of iterations are sufficient to guarantee a very accurate solution to the pressure equation starting from the initial value $v_0 = 1\,{\rm m^3/kg}$.

On the contrary, the equation for i (4.29) allows the direct determination of the dissociation and ionization in the gas for given thermodynamic conditions defined in terms of variables T and v. The gas pressure is calculated only subsequently from the values of T, v, α and i. From the numerical viewpoint, we have solved the fourth-order equation for i and that for $P_{\rm e}$ by means of Ferrari algorithm, see, e.g., [27], and have found that the solution of the former is much more stable numerically than the latter.

5 Equations of state of hydrogen gas/plasma

The equation of state of the energy is obtained from $E = F - T(\partial F/\partial T)_{V,\, N_{\rm H_2},\, N_{\rm H},\, N_{\rm p},\, N_{\rm e}}$ which yields the dimensionless specific energy $\epsilon = e/R_{\rm H_2} T_{\rm v}$,

$$\begin{aligned} \epsilon(t, v, \alpha, i) = {} & \tfrac{3}{2}(1 + \alpha + 2\alpha i)\, t \\ & + (1-\alpha)[\epsilon_{\rm rv}(t) - t_D] \\ & + 2(1-i)[\alpha\epsilon_{\rm H}(t/t_{\rm i}, v) - 1]\, t_{\rm i}, \end{aligned} \tag{5.1}$$

where $\epsilon_{\rm H}(\tau,v) = x_{\rm H}(\tau,v)/z_{\rm H}(\tau,v)$ with also $x_{\rm H}(\tau,v) = \tau^2\partial z_{\rm H}(\tau,v)/\partial\tau$.

The energy at zero temperature is $\epsilon_{\rm rv}(0) - t_D - 2t_{\rm i}$. It is therefore convenient to normalize the energy by adding the depth energy D_e of the Morse potential for all molecules, as well as the binding energy of all the hydrogen atoms $2t_{\rm i}$ with the electron in its ground state $n = 0$. The normalized energy is $\tilde\epsilon(t,v,\alpha,i) = \epsilon(t,v,\alpha,i) + t_D + 2t_{\rm i}$ and its final expression, indicated by the same symbol ϵ for notational simplicity, will be

$$\begin{aligned}\epsilon(t,v,\alpha,i) = {}& \tfrac{3}{2}(1+\alpha+2\alpha i)\,t \\ &+ (1-\alpha)\,\epsilon_{\rm rv}(t) + \alpha t_D \\ &+ 2\alpha[(1-i)\,\epsilon_{\rm H}(t/t_{\rm i},v) + i]t_{\rm i},\end{aligned} \tag{5.2}$$

so that at zero temperature $\epsilon(0) = \epsilon_{\rm rv}(0)$.

The specific entropy is obtained in a manner similar to the energy from the relation $S = -(\partial F/\partial T)_{V,\,N_{\rm H_2},\,N_{\rm H},\,N_{\rm p},\,N_{\rm e}}$ which gives its dimensionless counterpart $\sigma = s/R_{\rm H_2}$:

$$\begin{aligned}\sigma(t,v,\alpha,i) = {}& (1+\alpha+2\alpha i)\big(\tfrac{5}{2} + \tfrac{3}{2}\ln t\big) \\ &+ (1-\alpha)\left[\sigma_{\rm rv}(t) + \ln\left(\frac{v}{v_1}\right)\right] \\ &+ 2\alpha(1-i)\left[\sigma_{\rm H}(t/t_{\rm i},v) + \ln\left(\frac{v}{v_2}\right)\right] \\ &+ 4\alpha i\,\ln\left(\frac{v}{v_3}\right) + \Upsilon(\alpha,i) + \sigma_0,\end{aligned} \tag{5.3}$$

where the occurrence of the factor 4 in the third volumic term must be noted. Here $\sigma_{\rm H}(\tau,v) = \ln z_{\rm H}(\tau,v) + x_{\rm H}(\tau,v)/[\tau z_{\rm H}(\tau,v)]$, and

$$\begin{aligned} v_1^{-1} &= g^{\rm el}_{\rm H_2}\, m_{\rm H_2}\left(\frac{m_{\rm H_2} kT_{\rm v}}{2\pi\hbar^2}\right)^{\frac{3}{2}}, \\ v_2^{-1} &= g^{\rm n}_{\rm H}\, g^{\rm el}_{\rm H}\, m_{\rm H_2}\left(\frac{m_{\rm H}\, kT_{\rm v}}{2\pi\hbar^2}\right)^{\frac{3}{2}}, \\ v_3^{-1} &= 2m_{\rm H_2}\left(\frac{\sqrt{m_{\rm e}m_{\rm p}}\,kT_{\rm v}}{2\pi\hbar^2}\right)^{\frac{3}{2}}. \end{aligned} \tag{5.4}$$

Moreover, function $\Upsilon(\alpha,i)$ represents the mixing entropy of the dissociating and ionizing gas/plasma, which is found to be

$$\begin{aligned}\Upsilon(\alpha,i) \equiv {}& -(1-\alpha)\ln(1-\alpha) \\ &- 2\alpha(1-i)\ln[2\alpha(1-i)] - 4\alpha i\ln(2\alpha i).\end{aligned} \tag{5.5}$$

Note that $\Upsilon(\alpha,0) = \Upsilon_{\varsigma=2}(\alpha)$. The specific heat at constant volume $c_v = (\partial e/\partial T)_v$ is calculated from $e(T,v,\alpha,i)$ by

$$c_v = \left(\frac{\partial e}{\partial T}\right)_{\alpha,i} + \left(\frac{\partial e}{\partial \alpha}\right)_{T,i}\alpha_T(T,v) + \left(\frac{\partial e}{\partial i}\right)_{T,\alpha} i_T(T,v), \tag{5.6}$$

where the partial derivatives $\alpha_T = (\partial\alpha/\partial T)_v$ and $i_T = (\partial i/\partial T)_v$ are evaluated from system (4.25) by implicit differentiation. The specific heat at a constant pressure will be evaluated from $c_P = c_v - T(\partial P/\partial T)_v^2/(\partial P/\partial v)_T$ (for the pressure equation $P = P(T,v)$ see (6.2)). Moreover the relations

$$\epsilon'_{\rm rv}(t) = \frac{z_{\rm rv}(t)\,y_{\rm rv}(t) - x^2_{\rm rv}(t)}{[tz_{\rm rv}(t)]^2} \tag{5.7}$$

$$\frac{\partial\epsilon_{\rm H}(\tau,v)}{\partial\tau} = \frac{z_{\rm H}(\tau,v)\,y_{\rm H}(\tau,v) - x^2_{\rm H}(\tau,v)}{[\tau z_{\rm H}(\tau,v)]^2} \tag{5.8}$$

will be used, implying that the calculation of c_v requires the moments $y_{\rm rv}(t)$ and $y_{\rm H}(\tau,v)$ to assure a full consistency in the determination of the involved second derivative. Of course, the energy equation of state will be defined by $e(T,v) \equiv R_{\rm H_2}T_{\rm v}\,\epsilon(t,v,\alpha(t,v),i(t,v))$, with $t = T/T_{\rm v}$, and similarly for the entropy $s(T,v)$.

6 Comparisons

The curves of $c_v(T,v)$ are shown in Figure 6. For $T < 600\,{\rm K}$, the specific heat depends only on T but there are several curves which are valid only in the limit of low density and which correspond to different forms of the H_2 gas. The continuous curve is for the molecular hydrogen at equilibrium while the dashed and dot-dashed curves are for the ortho- and para-hydrogen forms, which are obtained by limiting the sum in (2.22) to odd or even j, respectively. The dotted curve of Figure 6 located between those of the ortho- and para-hydrogen corresponds to the experimental results, with the gas in a state of "frozen" metastable equilibrium consisting of $\frac{3}{4}$ ortho-hydrogen and $\frac{1}{4}$ para-hydrogen, as explained in [28, p. 472], such that

$$c_v^{\rm frozen} = \tfrac{3}{4}c_v^{\rm ortho} + \tfrac{1}{4}c_v^{\rm para}. \tag{6.1}$$

The four curves reported in Figure 6 for $T < 600\,{\rm K}$ are found in fair agreement with those given in [28, p. 471].

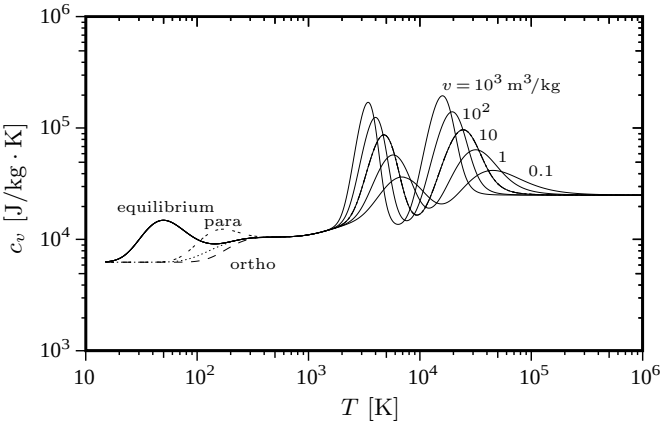

Fig. 6. Specific heat $c_v(T,v)$ as a function of temperature for different values of specific volume v in the hydrogen ideal gas/plasma model. The four different curves for $T < 10^3\,{\rm K}$ are valid only for low densities. In particular, the unlabeled dotted curve between the curves of the ortho- and para-hydrogen refers to the gas in a condition of "frozen" metastable equilibrium described by (6.1).

These curves of c_v are valid only for a low gas density, say $v > 3v_{\rm cr} = 0.1\,{\rm m}^3/{\rm kg}$, with $v_{\rm cr}$ denoting the critical specific volume of H_2: $v_{\rm cr} = 0.033\,{\rm m}^3/{\rm kg}$. Actually, for T about and less than 20 K, a dense H_2 becomes a liquid and undergoes a phase transition which is dependent on the para/ortho ratio. The failure of the ideal gas assumption at low temperatures and high densities implies that real gas effects must be included. However, the study of real gas effects in H_2 is beyond the scope of the present work and the reader interested in these effects in H_2 and in its allotrope forms of ortho- and para-hydrogen is referred to [29] and [30].

At higher temperatures the specific heat c_v depends also on v in consequence of dissociation and ionization. The curves of $c_v(T, v)$ for $v = 10^\ell\,{\rm m}^3/{\rm kg}$, $\ell = -1, 0, 1, 2, 3$ are shown in Figure 6: each has two distinct bells centered on the crossover temperatures, dependent on v, between the successive states, namely molecular, atomic and ionized.

In Figure 7 the values of $c_P(T)$ provided by the appoximate energy levels (2.12) in the range $T < 600\,{\rm K}$ have been compared to those calculated in [31] by means of the nonadiabatic eigenvalues of all bound and quasibound levels. The value of the proposed simple thermodynamic model based on the Harris&Bertolucci approximate spectrum of Morse rotating anharmonic oscillator are found to be very close to the accurate values of [31], with a maximum difference not exceeding 1% in the range $0 < T < 600\,{\rm K}$.

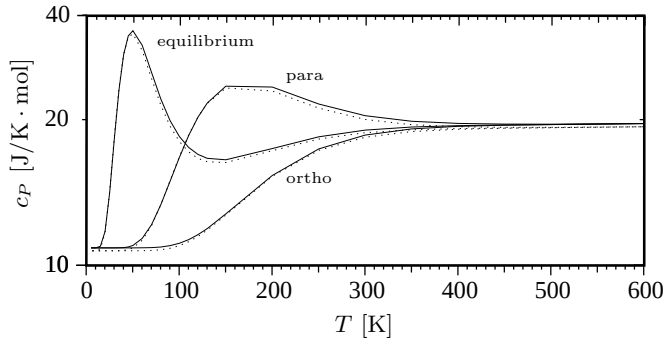

Fig. 7. Specific heat $c_P(T)$ of the three forms of H_2 ideal gas for low T and small density. Continuous curves from Harris–Bertolucci energy levels (2.12) and dotted curves from [31].

The specific heat at constant pressure has been compared also in the temperature range of ionization. In Figure 8 we plot the $c_P(T, P)$ as a function of T for three fixed values of pressure: $P = 0.01, 1, {\rm and} 100\,{\rm bar}$. The continuous curves refer to the present thermodynamic model while the dotted curves are reproduced from [20]. For the intermediate pressure the agreement is satisfactory but at the other two pressures the differences are larger.

The equilibrium dissociation and ionization predicted by the proposed model have been compared with the results from the monograph of Capitelli, Colonna and D'Angola [20]. For the fixed pressure $P = 1\,{\rm bar}$ the dimensionless partial pressures $P_{\rm H_2}/P, P_{\rm H}/P$ and $P_{\rm p}/P$ have been

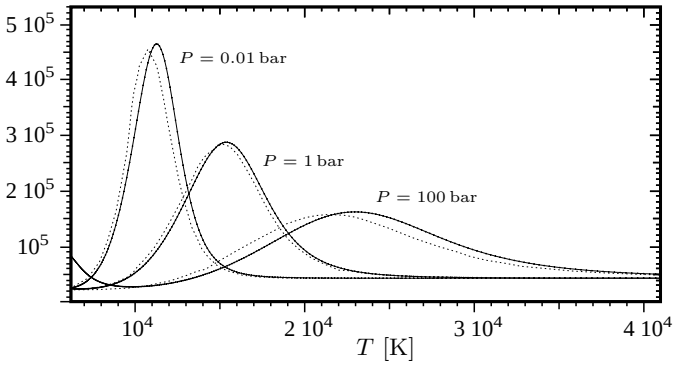

Fig. 8. Specific heat $c_P(T, P)$ in the range of temperatures involving hydrogen ionization, for some values of P. Continuous curve: present thermodynamic model. Dotted curves: Reference [20].

plotted by the continuous curves in Figure 9. The reference results [20, p. 12] are plotted as the dotted curves. The very small differences can be explained by the different temperature dependence in the equilibrium constants of the present model with respect to those in [20], which are exponential functions. At this low pressure the dissociation and ionization are to a good approximation independent phenomena and the exponential dependence on T is dominating over the other functions accounting for the translational energy of molecules and atoms, and for their internal structure through the involved partition functions.

For pressure $P = 100\,{\rm bar}$ the partial pressures are reported in Figure 10 and the result of the two models are found to be appreciably different. At this higher pressure the dissociation and ionization processes are coupled and rather different partial pressure at equilibrium are found. The disagreement can be attributed to the different temperature dependencies in the equilibrium constants, here by the functions of (4.26) and in [20] by purely exponential functions entering a single nonlinear equation for the electron pressure. The role of the more complex temperature dependence in the coupled regime has been verified by fixing the temperature in the functions other than the expo-

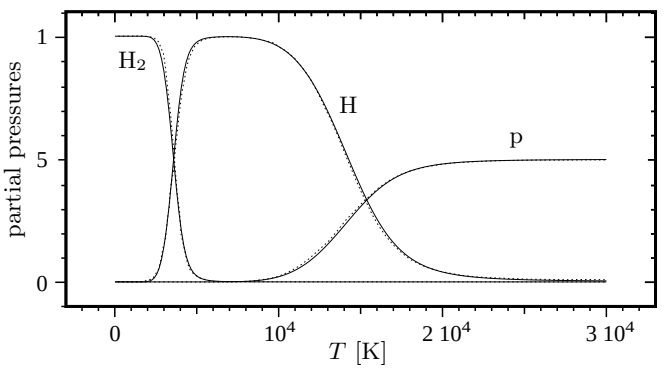

Fig. 9. Dimensionless partial pressures as a function of T with gas pressure $P = 1\,{\rm bar}$. Continuous curves: present work. Dotted curves: Reference [20].

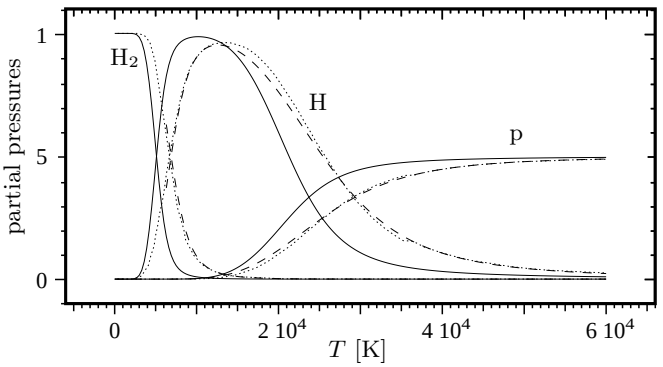

Fig. 10. Dimensionless partial pressures as a function of T with $P = 100\,\mathrm{bar}$. Continuous curves: present work. Dotted curves: Reference [20]. Dashed curves correspond to a merely exponential dependence on temperature in functions $\mathcal{D}$ and $\mathcal{I}$.

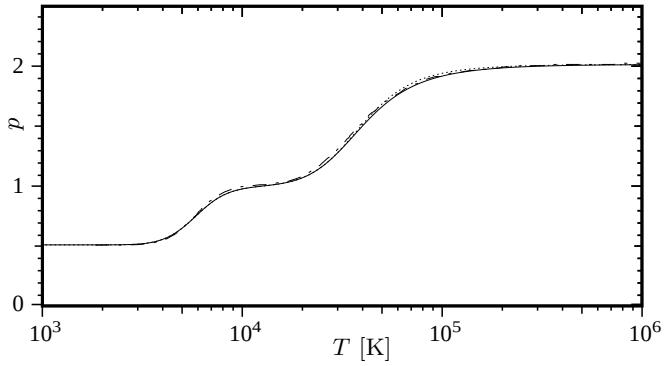

Fig. 11. Dimensionless pressure along the isochore $v = 1\,\mathrm{m}^3/\mathrm{kg}$. Continuous line: present work with Fermi cutoff (4.15). Dotted curve: present work with Zel'dovich truncation. Dot-dashed curve: method of Alastuey and Ballenegger [11].

nential of the proposed model. The corresponding partial pressures for a fixed value $T = 8000\,\mathrm{K}$ are plotted as the dashed curves in Figure 10. These curves are found to approximate fairly well the reference dotted curves of [20] in the full range of temperatures.

The behaviour of the thermodynamic model for the hydrogen gas/plasma proposed here is checked at low densities against the model of Alastuey and Ballenegger, in which the processes of recombination and formation of molecules and atoms is taken into account within the physical picture via the Ebeling function and a four-body partition function [11]. The comparison is done along the isochore $v = 1\,\mathrm{m}^3/\mathrm{kg}$ and considering the equation of state of pressure $P = -(\partial F/\partial V)_{T,\,N_{\mathrm{H}_2},\,N_{\mathrm{H}},\,N_{\mathrm{p}},\,N_{\mathrm{e}}}$:

$$P(T,v) = \left[1 + \alpha(T,v) + 2\alpha(T,v)\, i(T,v)\right] \frac{R_{\mathrm{H}_2} T}{v} \qquad (6.2)$$

made dimensionless with respect to its value in the purely molecular state, to give $p = P/(2R_{\mathrm{H}_2}T/v)$. The additional pressure term associated to the v-dependence of $z_{\mathrm{H}}(\tau, v)$ is negligible since these variations are extremely small. The pressure as a function of T is reported in Figure 11: the continuous line refers to the Fermi treament (4.16) to make the series of the atomic partition function convergent, the dotted curve is for the Zel'dovich cutoff (4.17), and the dash-point curve is drawn from the reference result of [11].

The temperatures of crossover between the molecular and atomic phases and between the atomic and ionized ones are predicted with comparable accuracy by the methods. Along the considerd isochore the ionized charges are weakly coupled and the present thermodynamic model with Fermi treatment reproduces the results of [11] for temperatures $T > 5 \times 10^4\,\mathrm{K}$ accurately. In this range the cutoff of Zel'dovich overestimates the reference value slightly. Both treatments give correct pressure values appreciably different from those of the Saha approximation in the region of nearly complete ionization, not reported in the figure, cf. [11]

To determine the limitation of the present model at higher densities due to not accounting for the electric interaction of the charges, we have calculated the pressure in the density range $1 < \rho < 10^3\,\mathrm{kg/m}^3$ at the three temperatures $T = 10^{4.1}\,\mathrm{K} = 1.2589 \times 10^4\,\mathrm{K}$, $T = 10^{4.5}\,\mathrm{K} = 3.1623 \times 10^4\,\mathrm{K}$ and $T = 10^{5.3}\,\mathrm{K} = 1.9953 \times 10^5\,\mathrm{K}$, considered by Poteckhin [32], as shown in Figure 12.

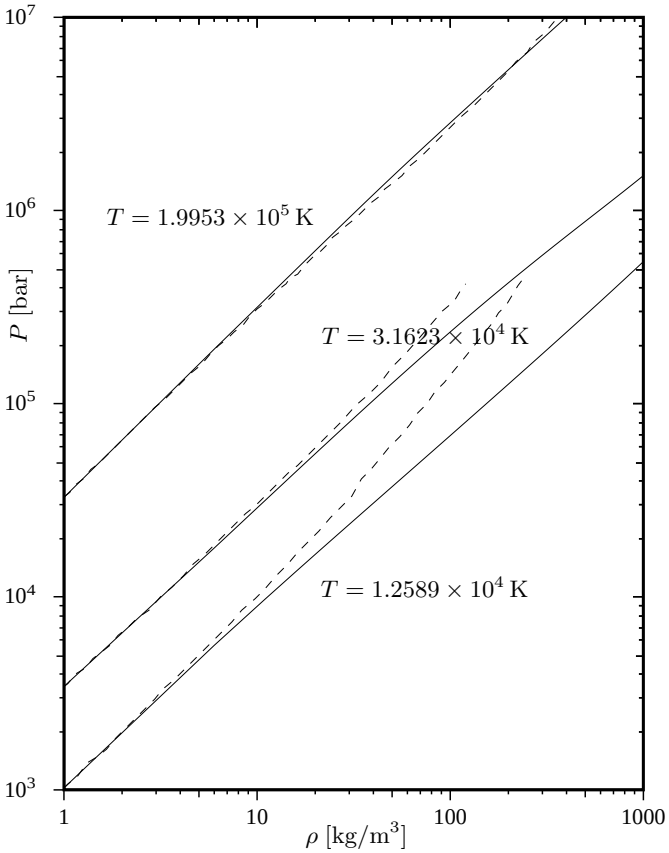

Fig. 12. Pressure as a function of density ρ for three temperatures $T = 10^{4.1}\,\mathrm{K} = 1.2589 \times 10^4\,\mathrm{K}$, $T = 10^{4.5}\,\mathrm{K} = 3.1623 \times 10^4\,\mathrm{K}$ and $T = 10^{5.3}\,\mathrm{K} = 1.9953 \times 10^5\,\mathrm{K}$. Continuous curves: present thermodynamic model. Dashed curves: occupation probability method for the hydrogen plasma of Poteckhin [32].

The pressure values in this range provided by the proposed method are compared with the values of the hydrogen plasma model of Poteckhin, which includes the effect of the electric interaction by means of an occupation probability method [32]. The plots in the Figure show the three isotherms in the ρ-P plane with logarithmic scales. The comparison of the two models for the highest temperature $T = 1.9953 \times 10^5\,\mathrm{K}$ shows clearly a fair agreement in the considered density range. At lower temperatures, the agreement is restricted to the domain of low densities; in particular, for $T < 10^4\,\mathrm{K}$ the electric interaction has substantial effects on pressure even at the intermediate density $\rho \approx 10\,\mathrm{kg/m^3}$, namely already for $v \le 0.1\,\mathrm{m^3/kg}$. The comparison shows that the proposed method is sufficiently accurate only in the limit of high temperatures and of low density, while it is unsuited to describe the thermodynamics of dense hydrogen at not high temperatures.

7 Gas/plasma model under classical rotations

For $T \gg T_\mathrm{r}$, the classical approximation for the molecular rotations of a homonuclear (symmetric) molecule $Z^\mathrm{rot}(T) = \frac{1}{2}T/T_\mathrm{r}$ can be exploited to avoid the calculation of the double sum of the roto-vibrational partition function $z_\mathrm{rv}(t)$ and replace it by the simpler function $z_\mathrm{v}(t)$. The partition function for the hydrogen molecule under the assumption of fully excited rotations is

$$Z^\star_{\mathrm{H}_2}(T,V) = \left(\frac{m_{\mathrm{H}_2}kT}{2\pi\hbar^2}\right)^{\frac{3}{2}} (g^\mathrm{n}_\mathrm{H})^2\,\frac{T}{2T_\mathrm{r}}\,z_\mathrm{v}(T/T_\mathrm{v}) \times g^\mathrm{el}_{\mathrm{H}_2}\,\mathrm{e}^{(D_e - E_{\mathrm{H}_2,0})/kT}\,V. \tag{7.1}$$

The (purely) vibrational partition function $z_\mathrm{v}(t)$ can be evaluated starting from either the "nonrotating" eigenvalues $E_{0,n}$, with $0 \le n \le 14$, of Pachucki and Komasa [13] or those of the nonrotating Morse oscillator, namely:

$$\frac{E^\mathrm{Morse}_n}{D_e} = -1 + \left[2 - \left(n+\tfrac{1}{2}\right)\chi_e\right]\left(n+\tfrac{1}{2}\right)\chi_e. \tag{7.2}$$

In the latter case, the partition function and its moments are defined quite simply by

$$\begin{bmatrix} z_\mathrm{v}(t) \\ x_\mathrm{v}(t) \\ y_\mathrm{v}(t) \end{bmatrix} \equiv \sum_{n=0}^{N_\mathrm{max}} \begin{bmatrix} 1 \\ a_n \\ a_n^2 \end{bmatrix} \mathrm{e}^{-a_n/t}, \tag{7.3}$$

where $N_\mathrm{max} = 1/\chi_e - \frac{1}{2}$ and $a_n = \left[1 - \left(n+\frac{1}{2}\right)\frac{\chi_e}{2}\right]\left(n+\frac{1}{2}\right)$. Using (7.1) with (4.19), the new dissociation equilibrium constant $K^\star_\mathrm{d}(T,v) = \frac{[Z_\mathrm{H}(T,V)/V]^2}{Z^\star_{\mathrm{H}_2}(T,V)/V}$ is found to be

$$K^\star_\mathrm{d}(T,v) = C^\star_\mathrm{d} \cdot (T/T_\mathrm{v})^{\frac{1}{2}}\,\mathrm{e}^{-T_D/T}\,\frac{z^2_\mathrm{H}(T/T_\mathrm{i},v)}{z_\mathrm{v}(T/T_\mathrm{v})}, \tag{7.4}$$

where

$$C^\star_\mathrm{d} = \frac{1}{\sqrt{2}}\,\frac{(g^\mathrm{el}_\mathrm{H})^2}{g^\mathrm{el}_{\mathrm{H}_2}}\,\frac{T_\mathrm{r}}{T_\mathrm{v}}\left(\frac{m_\mathrm{H}kT_\mathrm{v}}{2\pi\hbar^2}\right)^{\frac{3}{2}}, \tag{7.5}$$

since the nuclear spin multiplicity of H and H_2 in (4.19) and (7.1), respectively, cancel in the equilibrium constant, as usual in the approximation of fully excited rotations. Correspondingly, the definition (4.26) of function $\mathcal{D}(t,v)$ is replaced by

$$\mathcal{D}^\star(t,v) = \sqrt{t}\,\mathrm{e}^{-t_D/t}\,\frac{[z_\mathrm{H}(t/t_\mathrm{i},v)]^2}{z_\mathrm{v}(t)}\,\frac{v}{v^\star_\mathrm{d}} \tag{7.6}$$

with the new scale $v^\star_\mathrm{d}$ for the specific volume defined by

$$(v^\star_\mathrm{d})^{-1} = \frac{m_{\mathrm{H}_2}C^\star_\mathrm{d}}{4}. \tag{7.7}$$

The calculation yields $v^\star_\mathrm{d} = 0.3233 \times 10^{-3}\,\mathrm{m^3/kg}$. The new equation of state for the energy is obtained in the form

$$\begin{aligned}\epsilon^\star(t,v,\alpha,i) = {}& \tfrac{1}{2}(5+\alpha+6\alpha i)\,t \\ & + (1-\alpha)[\epsilon_\mathrm{v}(t) - t_D] \\ & + 2(1-i)\,[\alpha\epsilon_\mathrm{H}(t/t_\mathrm{i},v) - 1]\,t_\mathrm{i},\end{aligned} \tag{7.8}$$

where $\epsilon_\mathrm{v}(t) = x_\mathrm{v}(t)/z_\mathrm{v}(t)$. By adopting the same energy normalization employed before, the addition of $t_D + 2t_\mathrm{i}$ gives the quantity $\tilde\epsilon^\star = \epsilon^\star + t_D + 2t_\mathrm{i}$, and the final expression of the new normalized dimensionless energy, denoted by $\epsilon^\star$ for notational simplicity, reads

$$\begin{aligned}\epsilon^\star(t,v,\alpha,i) = {}& \tfrac{1}{2}(5+\alpha+6\alpha i)\,t \\ & + (1-\alpha)\,\epsilon_\mathrm{v}(t) + \alpha t_D \\ & + 2\alpha[(1-i)\,\epsilon_\mathrm{H}(t/t_\mathrm{i},v) + i]t_\mathrm{i}\end{aligned} \tag{7.9}$$

Here α and i are solution to the $\mathcal{D}^\star$-counterpart of system (4.25), through the solution of the quartic equation (4.29).

The new equation for the entropy reads

$$\begin{aligned}\sigma^\star(t,v,\alpha,i) = {}& \tfrac{1}{2}(5+\alpha+6\alpha i)(1+\ln t) + (1+\alpha+2\alpha i) \\ & + (1-\alpha)\left[\sigma_\mathrm{v}(t) + \ln\left(\frac{v}{v^\star_1}\right)\right] \\ & + 2\alpha(1-i)\left[\sigma_\mathrm{H}(t/t_\mathrm{i},v) + \ln\left(\frac{v}{v_2}\right)\right] \\ & + 4\alpha i\,\ln\left(\frac{v}{v_3}\right) + \Upsilon(\alpha,i) + \sigma^\star_0,\end{aligned} \tag{7.10}$$

where $\sigma_\mathrm{v}(t) = \ln z_\mathrm{v}(t) + x_\mathrm{v}(t)/tz_\mathrm{v}(t)$ and

$$(v^\star_1)^{-1} = \frac{(g^\mathrm{n}_\mathrm{H})^2\,g^\mathrm{el}_{\mathrm{H}_2}}{2}\,m_{\mathrm{H}_2}\,\frac{T_\mathrm{v}}{T_\mathrm{r}}\left(\frac{m_{\mathrm{H}_2}kT_\mathrm{v}}{2\pi\hbar^2}\right)^{\frac{3}{2}}, \tag{7.11}$$

while the constants v_2 and v_3 have already been defined in (5.4).

The two hydrogen gas models, one including the quantum treatment of rotation and the other assuming classical rotations, are compared by evaluating the sound speed by means of the well-known expression

$$c = \sqrt{\left(\frac{\partial P}{\partial\rho}\right)_s} = v\sqrt{\frac{T}{c_v}\left(\frac{\partial P}{\partial T}\right)^2_v - \left(\frac{\partial P}{\partial v}\right)_T}. \tag{7.12}$$

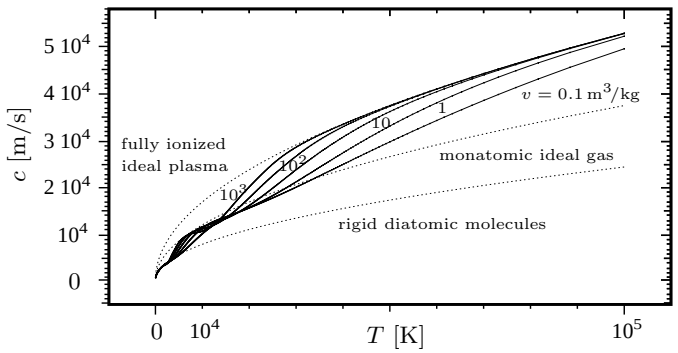

Fig. 13. Sound speed $c(T, v)$ as a function of T for different values of v. The dotted curves are for ideal gases with different specific heat ratios γ. Rigid diatomic molecule $\gamma_{\text{rig.dia.}} = \frac{7}{5}$. Monatomic: $\gamma_{\text{a}} = \frac{5}{3}$. Fully ionized ideal plasma: $\gamma_{\text{plasma}} = \frac{10}{3}$.

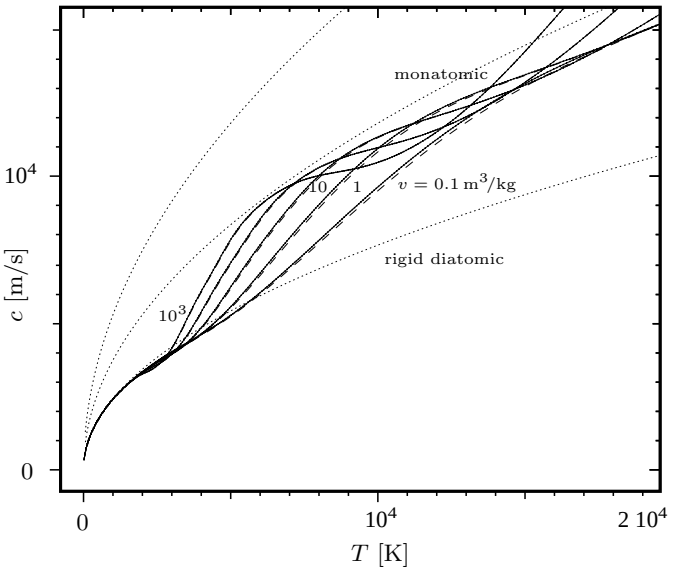

Fig. 14. Sound speed $c(T, v)$ in the temperature range of dissociation for different values of v. Continuous curves: general thermodynamic gas/plasma model (5.2)–(5.3). Dashed curves: simpler model under classical rotations (7.9)–(7.10). The meaning of the dotted curves is as in Figure 13.

The values of $c(T, v)$, based on the general gas/plasma model described in section 5, are shown in Figure 13 for different values of v. At low temperatures, the sound speed of the hydrogen gas coincides with that of a diatomic ideal gas with rigid molecules, with $\gamma_{\text{rig.dia.}} = \frac{7}{5}$, namely $c_{\text{rig.dia.}}(T) = \sqrt{(7/5)R_{\text{H}_2}T}$, for any density. Then, for $T > 1000\,\text{K}$, the molecular oscillations come into play and make the dissociation possible, so that the sound speed depends also on v. About $T \approx T_{\text{v}}$ the dissociation tends to be complete and the gas becomes monatomic, so all curves tend to one and the same sound speed curve of the monatomic gas $c_{\text{a}}(T) = \sqrt{\gamma_{\text{a}}R_{\text{H}}T} = \sqrt{(10/3)R_{\text{H}_2}T}$. For higher T, the ionization sets in and the sound speed of the partially ionized gas depends substantially on its density, but tends uniformly to the limit value $c_{\text{plasma}}(T) = \sqrt{\gamma_{\text{a}}2R_{\text{H}}T} = 2\sqrt{(5/3)R_{\text{H}_2}T}$ which corresponds to a monatomic gas with an average atomic mass half of that of H, the electron mass being negligible with respect to the proton one.

Figure 14 contains an enlargement of the curves of Figure 13 in the range of low temperatures and for the same density values. The sound speed of the general thermodynamic model (continuous curves) are compared to that of the simplified gas/plasma model under classical rotations described in this section (dashed curves). The two models are found to agree fairly well at the lower densities and the differences do not exceed a few % at the highest considered density of $v = 0.1\,\text{m}^3/\text{kg}$, confirming the adequacy of the simpler model for gasdynamic applications.

As a last demonstration of the suitability of the proposed thermodynamic model of the hydrogen gas/plasma for applications in computational fluid dynamics, we determine the Rankine–Hugoniot adiabats for shock waves involving dissociation and ionization. Since the equations of state $e(T, v)$ and $P(T, v)$ in (7.9) and (6.2) are available, the Hugoniot relation is written in the form

$$e(T, v) - e_0 + \tfrac{1}{2}[P_0 + P(T, v)](v - v_0) = 0 \qquad (7.13)$$

which represents an implicit definition of the function $v = v^{\text{RH}}(T)$ along the Rankine–Hugoniot adiabat. This nonlinear equation can be solved by Newton method. Figure 15 contains the curves of the irreversible adiabats $P = P^{\text{RH}}(v) \equiv P(T^{\text{RH}}(v), v)$, issuing from several initial states, all with $v_0 = 10^3\,\text{m}^3/\text{kg}$ but for different dimensionless temperatures $t_0 = T_0/T_{\text{v}} = 0.05,\ 0.1,\ 0.25,\ 0.5,\ 1,\ 2,\ 2.5,\ 3,\ 5$.

Differently from the ordinary Rankine–Hugoniot adiabats of an ideal gas, which are always monotonic curves, the adiabats in hydrogen may have one or three local extrema (function $v = v^{\text{RH}}(P)$) depending on the initial state, due to the fact that the pre-shock hydrogen conditions may be very different. In fact, the gas can be initially either fully molecular, or mainly atomic after a great dissociation, or also in a prevalently ionized state. According to each of these initial conditions, shocks of increasing intensity may or may not involve dissociation or ionization or both. This is at the origin of the very different behaviours of the hydrogen adiabats shown in Figure 15. In particular, the lowest curve starts at the smallest initial temperature $T_0 = 315\,\text{K}$ and the gas compression initially follows the standard hyperbolic curve with $P \to \infty$ tending to a vertical asymptote.

Three different possible asymptotes are plotted in the figure as dotted vertical lines. They correspond to the lower bound for the ratio $v^{\text{asympt}}/v_0 = (\gamma - 1)/(\gamma + 1)$ that the adiabat cannot overcome, since $P \to \infty$, for three possible ideal gas models. The first asymptote on the right in the figure corresponds to a monatomic gas with $\gamma_{\text{a}} = \frac{5}{3}$ and the value $(v^{\text{asympt}}/v_0)_{\text{a}} = \frac{1}{4}$. The second intermediate asymptote corresponds to a diatomic ideal gas with rigid molecules and fully excited rotations such that $\gamma_{\text{rig.dia.}} = \frac{7}{5}$ and $(v^{\text{asympt}}/v_0)_{\text{rig.dia.}} = \frac{1}{6}$. The third asymptote, on the left, corresponds to a diatomic ideal gas with fully excited rotations and vibrations so that $\gamma_{\text{vib.dia.}} = \frac{9}{7}$ and $(v^{\text{asympt}}/v_0)_{\text{vib.dia.}} = \frac{1}{8}$.

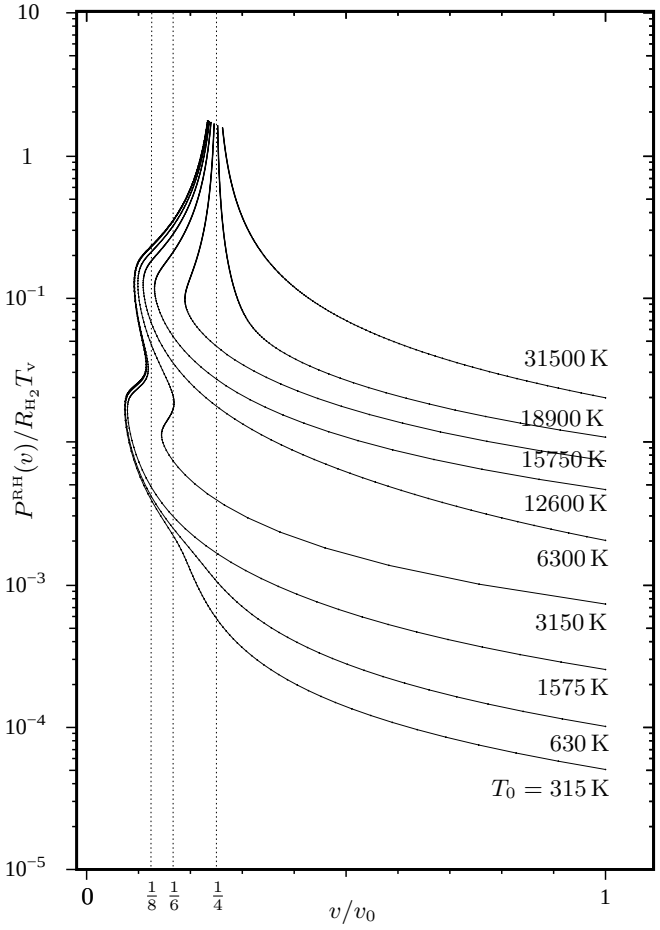

Fig. 15. Post-shock pressure $P^{\mathrm{RH}}(v)/R_{\mathrm{H}_2}T_{\mathrm{v}}$ scaled in density units of kg/m^3 along several Rankine–Hugoniot adiabats as a function of the ratio v/v_0. Shock waves in hydrogen gas/plasma may cause dissociation and/or ionization: initial states with $v_0 = 10^3$ m^3/kg and with different values of the initial temperature T_0.

The compression adiabat lowest in the figure tends initially toward the most left asymptote $(v^{\mathrm{asympt}}/v_0)_{\mathrm{vib.dia.}} = \frac{1}{8}$, but, for higher P and T, the curve deviates as a consequence of molecular dissociation. The dissociable molecular hydrogen can become denser than permitted to its undissociable ideal counterpart. The dissociation proceeds further and a condition is reached in which compression and temperature can increase while the gas density decreases: the molecular dissociation allows an augmentation of the internal energy at a lower density due to duplication of the number of particles with their kinetic energy. At higher and higher compression and temperature, the atomic hydrogen starts to ionize and the adiabatic curve has a behaviour similar to that found in the dissociation zone. Eventually, for extremely strong compressions, the curve tends to the first vertical asymptote $(v^{\mathrm{asympt}}/v_0)_{\mathrm{a}} = \frac{1}{4}$ pertaining to an atomic gas. However, it must be noted that the adiabat tends to the monatomic asymptote from the left side, and not from right side, as occurs in a truly monatomic ideal gas.

Considering now different adiabats with higher initial temperatures $T_0 = 630\,\mathrm{K}$ and $T_0 = 1575\,\mathrm{K}$, their behaviour is very similar to the first one, with three similar local extrema, since the initial dissociation degree of the gas in the two initial conditions is very small, $\alpha_0 \approx 0$ and $\alpha_0 \approx 0.22 \times 10^{-4}$, respectively. The initial temperature of the fourth adiabat is $T_0 = 3150\,\mathrm{K}$ with $\alpha_0 = 0.43$ and $i_0 = 0$ and the three local extremes are still present since the dissociation has still to play an essential part of its role, while the distance between the first minimum and the local maximum is decreasing.

The next adiabat starts at $T_0 = 6300\,\mathrm{K}$ with an initial dissociation almost complete, $\alpha_0 = 0.998$ and a rather small initial ionization $i_0 \approx 0.16 \times 10^{-4}$. The corresponding curve has only one local extremum due to the ionization occurring for increasing compression. This behaviour is shared also by the next two adiabats starting at $T_0 = 12600\,\mathrm{K}$ and $T_0 = 15750\,\mathrm{K}$, which are characterized by an appreciable initial ionization of $i_0 = 0.133$ and $i_0 = 0.44$, respectively. These adiabats involving a progressive ionization toward the fully ionized state tend to the monatomic asymptote still from the left.

For the last two adiabats starting at the relatively high temperatures $T_0 = 18900\,\mathrm{K}$ and $T_0 = 31500\,\mathrm{K}$, the initial ionization is higher $i_0 = 0.75$ and $i_0 = 0.98$ and the curves have the usual monotonic behaviour, with the graph tending to the atomic vertical asymptote, this time from the right, as in any ideal gas.

8 Conclusions

We have presented a simple approximate thermodynamic model for the hydrogen gas including the possibility of molecular dissociation into neutral atoms and of their ionization to form a gas/plasma. The physical model is restricted to the regime of low densities and assumes that the system consists of an ideal gas mixture of free non-interacting particles. While this assumption is adequate in representing molecular dissociation under diluted conditions, it fails when ionization occurs, since the electric interaction between the charges is always present at any density and temperature. However, for low densities up to the moderate density $\rho \approx 1\,\mathrm{kg/m^3}$, the ionized charges remain weakly coupled [12, p. 216] and the ideal gas approximation can be accepted.

The proposed model is based on either the very accurate spectrum of the roto-vibrational states of the molecular hydrogen calculated recently by Pachucki and Komasa [13] or the energy levels derived from the Morse rotating oscillator by Harris and Bertolucci [14]. The latter levels are given by a simple closed-form analytical expression, that has been shown to provide an internal partition function of H_2 approximating rather closely that derived from Pachucki and Komasa energy levels, to the point of giving virtually indistinguishable equations of state. Thus the two spectra provide alternative descriptions equally suitable for thermodynamic purposes.

In the model, the degree of dissociation and ionization α and i are determined by solving a very simple system of

two coupled second order equations, with coefficients dependent on the thermodynamic state of the gas. The system reduces to a single fourth order equation for i which has been found to have only one physically admissible solution $i \in [0, 1]$ for densities in the range $v > 10^{-5}\,\mathrm{m}^3/\mathrm{kg}$ and for $T < 10^6\,\mathrm{K}$; for higher temperatures, a solution i extremely near to 1 is easily selected as the proper one among three admissible real values.

The equations of state for energy, entropy and specific heat have been given in closed form as analytical expressions which are useful for representing the thermodynamical processes encountered in fluid dynamic applications such as, for example, the Hugoniot adiabats and the rarefaction waves. This thermodynamic model is very crude since it is based on the ideal gas hypotesis and disregards completely the Coulomb interactions in the plasma state. The model is therefore limited to low densities and it excludes also molecular ionization and negative ion formation. However the model encompasses the full range of temperatures, from very low, where both ortho- and para-hydrogen forms of the gas may manifest, through the intermediate values where molecular dissociation sets in, up to the high temperatures of partial and eventually full ionization.

The values of pressure in the presence of dissociation and ionization at equilibrium have been compared with those calculated by recent refined models formulated in the framework of the physical picture [11] and of the chemical picture [32]. The comparison of pressure values provided by pressure equation proposed in this work with those given by the two more refined models has shown that for moderate densities not higher than $\rho \simeq 1\,\mathrm{kg}/\mathrm{m}^3$ the new simple thermodynamic model is of a comparable accuracy. This confirms the potentialities of the proposed thermodynamic model for numerical simulations of supersonic and hypersonic flows of the hydrogen at thermodynamical and chemical equilibrium, cf. *e.g.* [33].

Acknowledgements. The authors are grateful to the reviewers for their valuable comments and are pleased to thank Laura Dalzini for her assistance in the reproduction of some graphical results as well as in the creation of the graphical abstract. The first author is indebted to Joshua Fetching and to all members of FdVS for insightful discussions and continuing support.

References

1. H. B. Callen, *Thermodynamics and an Introduction to Thermostatistics*, John Wiley & Sons, New York, 1988.
2. R. Kubo, *Statistical Mechanics*, North-Holland Publishing Company, Amsterdam, 1965.
3. J. Lighthill, J. Fluid Mechanics, **2**, **1**, (1957) 1–32.
4. W. G. Vincenti and C. H. Kruger, *Introduction to Physical Gas Dynamics*, John Wiley, New York, 1965.
5. P. M. Morse, Phys. Rev., **34**, (1929) 57–64.
6. F. J. Gordillo-Vázquez and J. A. Kunc, J. Appl. Phys., **84**, **9**, (1998) 4693–4703.
7. L. D. Landau and E. M. Lifshitz, *Statistical Physics*, Part. 1, Elsevier, Oxford, 1980.
8. D. G. Hummer and D. Mihalas, Astrophysical J., **331**, (1988) 794–814.
9. D. Mihalas, W. Däppen and D. G. Hummer, Astrophysical J., **331**, (1988) 815–825.
10. A. Alastuey, V. Ballenegger, F. Cornu and Ph.A. Martin, J. Stat. Phys., **130**, (2008) 1119–1176.
11. A. Alastuey and V. Ballenegger, Contrib. Plasma Phys., **52**, (2012) 95–99.
12. Ya. B. Zel'dovich and Yu. P. Raizer, *Physics of Shock Waves and High-Temperature Hydrodynamic Phenomena*, Academic Press, New York, 1967.
13. K. Pachucki and J. Komasa, J. Chem. Phys., **130**, 164113 (2009).
14. D. C. Harris and M. D. Bertolucci, *Symmetry and Spectroscopy*, Dover, New York, 1989.
15. E. Fermi, Zs. Phys., **26**, (1924) 54–56.
16. Y. Babou, Ph. Rivière, M.-Y. Perrin and A. Soufiani, Int. J. Thermphys., **30**, (2009) 416–438.
17. G. A. Blake, `www.gps.caltech.edu/g̃ab/ch21b/lectures/lecture07.pdf`, Lecture # 7, Vibration-Rotation Spectra of Diatomic Molecules (2009).
18. G. V. Yukhnevich, *Doklady Physics*, **45**, **5**, (2000) 201–204.
19. D. Bruno, F. Esposito and V. Giovangigli, J. Chem. Phys., **138**, (2013) 084302.
20. M. Capitelli, G. Colonna and A. D'Angola, *Fundamental Aspects of Plasma Chemical Physics: Thermodynamics*, Springer, New York, 2011.
21. J. M. L. Martin, J. P. Francois and R. Gijbels, J. Chem. Phys., **96**, (1992) 7633–7645.
22. G. Emanuel, *Advanced Classical Thermodynamics*, AIAA Education Series, Washington, D.C., 1987.
23. W. Grimus, `arXiv:1112.3748v1 [physics.hist-ph] 16 Dec 2001.`
24. M. R. Zaghloul, Phys. Plasmas, **17**, (2010) 062701.
25. A. Y. Potekhin, Phys. Plasmas, **17**, (2010) 124705.
26. M. R. Zaghloul, Phys. Plasmas, **17**, (2010) 124706.
27. Don Herbison-Evans, Technical Report TR94-487, Basser Department of Computer Science, University of Sydney, Australia, Updated 31 March 2011.
28. T. L. Hill, *Statistical Mechanics, Principles and Selected Applications*, Dover, New York, 1987.
29. R. T. Jacobsen, J. W. Leachman, S. G. Penoncello and E. W. Lemmon, Int. J. Thermophys., **28**, **3**, (2007) 758–772.
30. J. W. Leachman, R. T. Jacobsen, S. G. Penoncello and E. W. Lemmon, J. Phys. Chem. Ref. Data, **38**, **3**, (2009) 721–748.
31. R. J. Le Roy, S. G. Chapman and F. R. W. McCourt, J. Phys. Chem., **94**, (1990) 923–929.
32. A. Y. Poteckhin, Phys. Plasmas, **3**, (1996) 4156–4165.
33. M. MacLean, A. Dufrene, T. Wadhams and M. Holden, AIAA Paper, (2010) 2010–1562.